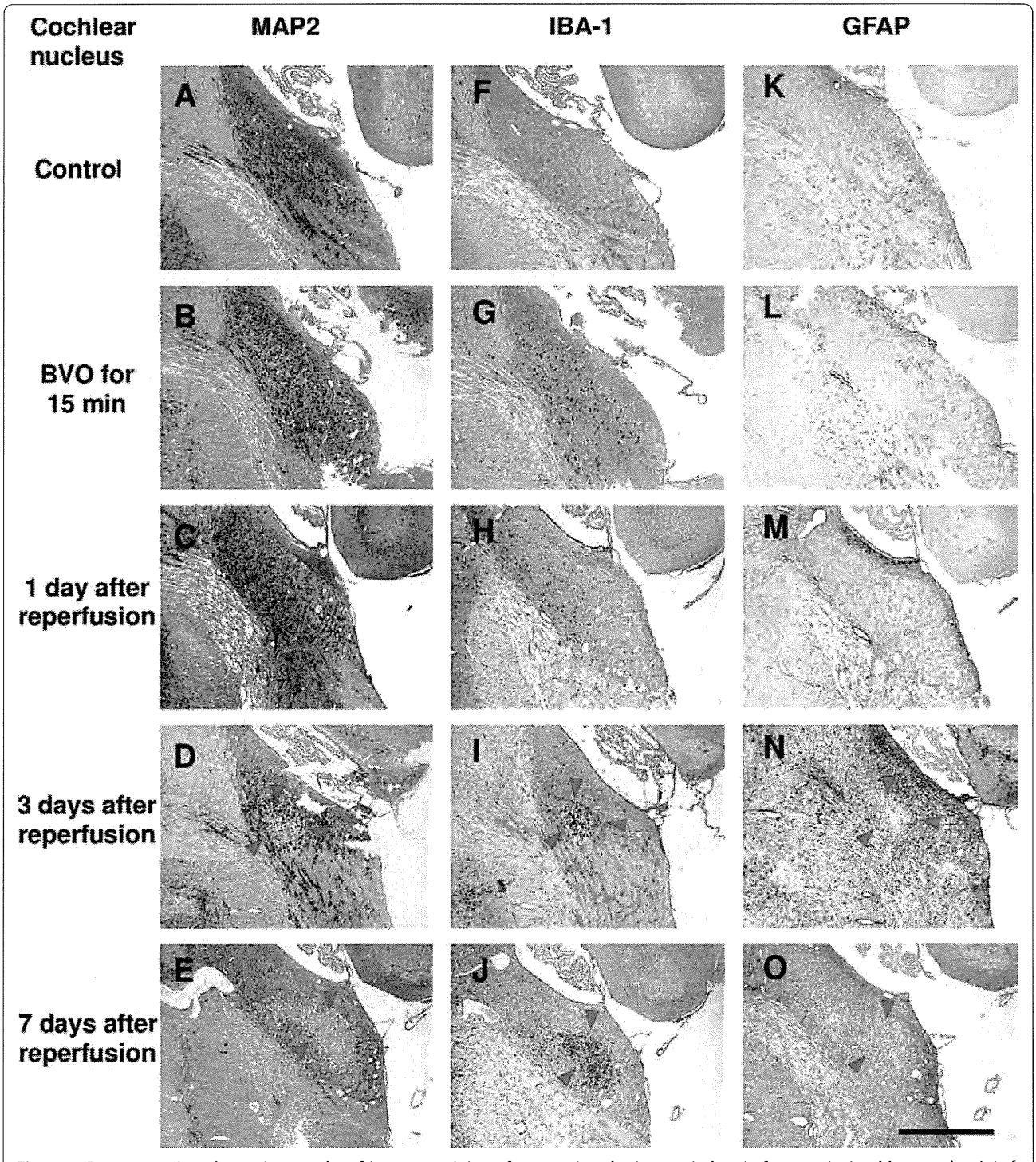

Figure 4 Representative photomicrographs of immunostaining after transient brainstem ischemia for 15 min (cochlear nucleus). Left column shows immunoreactivity for MAP2 (A-E); middle column shows immunoreactivity for IBA-1 (F-J); right column shows immunoreactivity for GFAP (K-O). Ischemic lesions with loss of immunoreactivity for MAP2 were seen in the ventral cochlear nucleus (VC) at 3 days and 7 days after reperfusion (D and E; red arrowheads). Clusters of IBA-1-positive amoeboid microglia/macrophages (I and J; red arrowheads) and loss of GFAP expression (N and O; red arrowheads) were detected in the same areas where MAP2 expression was lost at 3 days and 7 days after reperfusion. Increased immunoreactivity for GFAP (N and O; red arrowheads) was also detected around ischemic lesions at 3 days and 7 days after reperfusion. Scale bars = 0.5 mm.

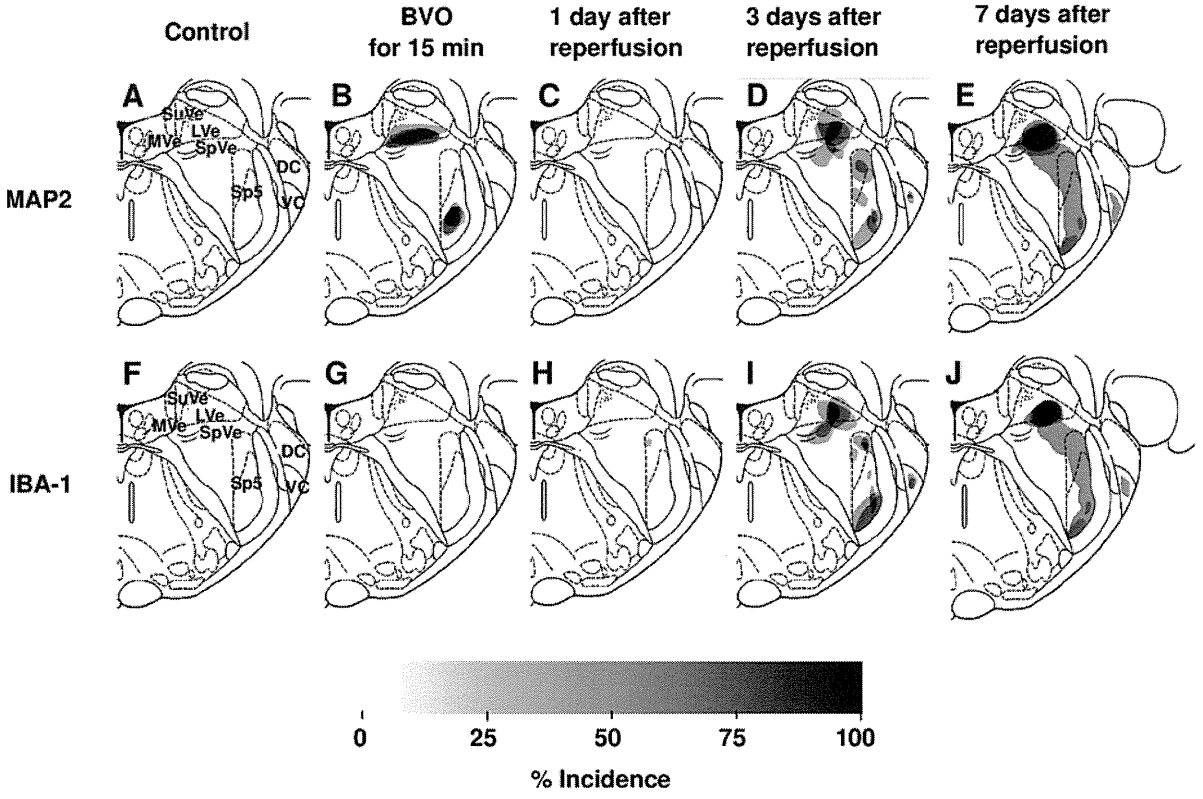

Figure 5 Incidence maps of immunoreactivity for MAP2 (decrease) and IBA-1(increase) in coronal gerbil brain sections at various times after transient brainstem ischemia for 15 min (at level of pons [5.5 mm caudal to bregma]). Areas of altered immunoreactivity were outlined in all animals examined and superimposed to represent the incidence map (%). For details, see text.

GFAP immunoreactivity disappeared in the central part of ischemic lesions where MAP2 immunostaining was lost. Immunoreactivity for GFAP increased in the periphery of ischemic lesions as well as the neighboring areas around ischemic lesions. These results suggested that reactive astrocytes proliferated in the neighboring areas around ischemic lesions and migrated into the ischemic lesions. A reduction of GFAP staining was detected in LVe (blue arrows in Figures 1O and 2O) and the ventral part of Sp5 (red arrows in Figures 1O and 3O) in all 3 animals (100%). A reduction of GFAP staining was also detected in the dorsal part of Sp5 (blue arrowheads in Figures 1O and 3O) and the ventral cochlear nucleus (VC) (red arrowheads in Figures 1O and 4O) in 1 out of 3 animals (33%).

Temporal profile of ischemic lesions

The total area of ischemic lesions detected by MAP2 staining in each animal was calculated and summarized in Figure 6. Just after brainstem ischemia for 15 min, the total area of ischemic lesions was 0.33 ± 0.041 [Mean ± SD] (mm^2). Although ischemic lesions disappeared one day after brainstem ischemia, evolution of ischemic lesions was detected 3 and 7 days after

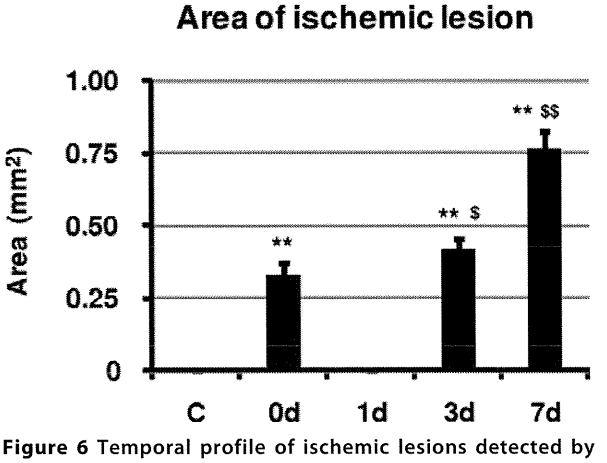

Figure 6 Temporal profile of ischemic lesions detected by MAP2 staining after transient brainstem ischemia for 15 min. The area of ischemic lesions detected by MAP2 staining in each animal was calculated. For details, see text. C: control, 0 d: just after brainstem ischemia for 15 min, 1 d, 3 d and 7 d: 1, 3 and 7 days after transient brainstem ischemia for 15 min, respectively. All values are given as mean ± SD. Differences were analyzed using one-way ANOVA followed by Bonferroni's multiple comparison test. A p value of less than 0.05 was considered to indicate statistical significance. ** and $$ indicate significant ($p < 0.01$) difference vs. C and 0 d, respectively. $ indicates significant ($p < 0.05$) difference vs. 0 d.

transient brainstem ischemia (0.42 ± 0.034 and 0.76 ± 0.064, respectively).

Discussion

Detection of morphological damage in early cerebral ischemia is difficult with conventional histological procedures including triphenyltetrazolium chloride and hematoxylin-eosin staining. With these conventional methods, morphological evidence of neuronal death does not become apparent until 1 to 2 hours after the onset of cerebral ischemia. However, early ischemic lesions can now be detected by applying immunohistochemical methods, and a reduction in microtubule-associated protein 2 (MAP2) immunoreactivity has been found to be an early, sensitive marker of ischemic neuronal damage [6]. In our study, by using this method, we showed that the lateral vestibular nucleus (LVe) and the ventral part of the spinal trigeminal nucleus (vSp5) were particularly vulnerable to ischemia.

In the LVe, multipolar giant neurons (Deiter's neurons) were most vulnerable to ischemia. Vestibular neurons receive excitatory glutaminergic input from the vestibular nerve [7] and commissural excitatory afferents [8]. Immunohistochemical and in situ hybridization histochemical studies revealed the highest glutamate receptor 2 (GluR2) expression in giant Deiter's neurons of the lateral vestibular nucleus and the lowest expression in small neurons throughout the vestibular nuclei [9]. These reports suggest that Deiter's neurons receive excitatory input and have selective sensitivity to excitotoxicity. As an analogy to hippocampal neurons [10], we speculate that an ischemia-induced alteration of GluR2 expression in Deiter's neurons induced cell death. Although further investigations are required to clarify the mechanisms underlying this selective vulnerability and delayed neuronal damage, they may also be related to several other factors such as the degree of cerebral hypoperfusion after reperfusion [11], inhibition of protein synthesis [12], neutrophil infiltration following reperfusion [13], free radical production [14], dysfunction of the mitochondrial shuttle system [15] or apoptosis [16].

Furthermore, we showed that the ischemic lesions in LVe and vSp5 had disappeared one day after reperfusion, but appeared again three days after reperfusion and thereafter. The observed loss of immunoreaction for MAP2 may reflect cytoskeletal breakdown, because MAP2 is involved in maintaining the structural integrity of the neuronal cytoskeleton [17]. The ischemia-induced rapid elevation of intracellular Ca^{2+} concentration and subsequent activation of Ca^{2+}-dependent phosphatases (e.g., calcineurin) and proteases (e.g., calpains) can lead to dephosphorylation and proteolytic degradation of MAP2 [18,19]. Therefore, ischemia-induced loss of immunoreaction for MAP2 is considered to be a reliable marker of neurons that are already undergoing irreversible processes in cell death [20]. However, Kitagawa et al. showed that loss of MAP2 immunostaining preceded the development of overt neuronal loss in a gerbil model of transient forebrain ischemia [6]. Our results are also consistent with this notion that MAP2 immunostaining can be used as an indicator of still viable neurons that will undergo irreversible injury only at a later time point.

We also demonstrated clusters of IBA-1-expressing cells in the ischemic lesions where MAP2 staining was lost three days after ischemia and thereafter. The rat *Iba1* gene has been identified as a microglia-specific transcript [21]. The isolated *Iba1*clone was 0.8 kb, a rather small cDNA encoding a 17-kDa protein consisting of 147 amino acids. IBA-1 is an interferon-γ (IFN-γ)-inducible Ca^{2+}-binding EF-hand protein that is encoded within the HLA class III genomic region. Expression of IBA-1 is mostly limited to the monocyte/macrophage lineage, and is augmented by cytokines such as IFN-γ. It was assumed that IBA-1 is a novel molecule involved in inflammatory responses and allograft rejection, as well as activation of macrophages [22]. In the normal brain, IBA-1 is highly expressed in resident microglial cells, but is never expressed in neurons and astrocytes [22]. After ischemia, IBA-1 is also expressed in activated resident microglial cells and infiltrating hematogenous macrophages [23,24].

Resident microglial cells rapidly became activated after ischemia. They developed amoeboid or rounded cell bodies and migrated rapidly into the ischemic lesion. For example, IBA-1 expression was rapidly up-regulated in the gerbil hippocampal CA1 region at 30 min after transient forebrain ischemia for 5 min [25]. However, microglial cells did not proliferate rapidly. Denes et al. showed that resident microglial cells exhibited intense proliferation at 48 and 72 h after transient occlusion of the middle cerebral artery (MCA) in the mouse. Average microglial cell number in the ischemic lesion did not increase significantly up to 48 h after transient ischemia [26]. We also demonstrated that a significant increase in Iba-1-positive cells was not detected in the ischemic cortex of the rat until one day after permanent MCA occlusion (MCAO), while a significant decrease in Iba-1-positive cells was detected even 2 h after permanent MCAO[27]. Furthermore, infiltrating hematogenous macrophages do not appear in the brain within one day after ischemia [24]. In this study, we did not detect clusters of IBA-1-expressing cells (i.e. topical proliferation of microglial cells) within one day after ischemia. Clusters of IBA-1-expressing cells initially appeared in the core of the ischemic lesions three days after ischemia, and these IBA-1-positive cells exhibited round cell bodies

and possessed pseudopodia and thin filopodia-like processes, indicating a motile phagocytic phenotype. At seven days after ischemia, IBA-1-expressing cells with an amoeboid shape were distributed more peripherally in the ischemic lesions as well as in the core of the ischemic lesions. Based on their morphological features and the temporal profile of the distribution of IBA-1-positive cells in ischemic lesions, we speculated that these IBA-1-expressing cells were of hematopoietic origin, although we could not exclude the possibility that they were of resident microglial origin.

In addition, we showed that delayed progression of ischemic neural death took place in the brainstem. Although other morphological and biochemical investigations including electron microscopic study are required for further analysis, this delayed neuronal damage in the brainstem is reminiscent of the delayed neuronal death in the hippocampus after transient forebrain ischemia [5]. There is increasing evidence that microglial cells contribute to delayed neuronal death. Recruitment and activation of microglial cells gradually increase within the hippocampal CA1 area over 24 h after transient forebrain ischemia, before the degeneration of neurons [28]. Endangered neurons can release proinflammatory chemokines such as monocyte chemoattractant protein-1 (MCP-1/CCL2) and secondary lymphoid-tissue chemokine (SLC/CCL21). Expression of MCP-1 and SLC is increased in neurons after ischemia [29,30]. Subsequently, recruited and activated microglial cells produce inflammatory mediators, including interleukin-1β (IL-1β), tumor necrosis factor-α (TNF-α), and nitric oxide (NO), which contribute to delayed neuronal death [31]. Moreover, immunosuppressants, such as FK506, prevent microglial activation and neuronal damage after ischemia [32]. Consistent with these findings, our results also suggest that activated microglia/macrophages play a crucial role in this delayed neuronal cell death in the brainstem.

Conclusions

In conclusion, we evaluated the evolution of ischemic lesions in the brainstem after transient brainstem ischemia in gerbils. Using immunostaining for MAP2, ischemic lesions were detected in LVe and vSp5 in all four animals. These ischemic lesions disappeared one day after reperfusion, but appeared again three days after reperfusion and thereafter in all animals examined. In addition, clusters of activated microglia/macrophages were detected in these ischemic lesions three days after ischemia and thereafter. These results suggest that delayed neuronal cell death took place in the brainstem after transient brainstem ischemia in gerbils.

Abbreviations

SuVe: superior vestibular nucleus; MVe: medial vestibular nucleus; LVe: lateral vestibular nucleus; SpVe: spinal vestibular nucleus; DC: dorsal cochlear nucleus; VC: ventral cochlear nucleus; Sp5: spinal trigeminal nucleus; BVO: bilateral vertebral artery occlusion

Acknowledgements

This project was supported, in part, by grants from the Ministry of Education, Science, Sports and Culture of Japan. We are grateful for the secretarial assistance of Ms. K. Hiraoka.

Author details

[1]Department of Functional Histology, Ehime University Graduate School of Medicine, Shitsukawa, Toon, Ehime 791-0295, Japan. [2]Department of Otolaryngology, Ehime University Graduate School of Medicine, Shitsukawa, Toon-shi, Ehime 791-0295, Japan.

Authors' contributions

The original concept was by RH, MS and KG. Animal experiments were performed by ST and TY. Immunostaining was performed by FC and PZ. Evaluation of immunostaining was performed by FC, RH and NH. The manuscript was written and edited by FC and RH. All authors read and approved the final manuscript.

Competing interests

The authors declare that they have no competing interests.

Received: 21 March 2010 Accepted: 14 September 2010
Published: 14 September 2010

References

1. Auer RN, Benveniste H: *Hypoxia and related conditions* New York: Oxford University Press 1998.
2. Pulsinelli WA, Brierley JB, Plum F: **Temporal profile of neuronal damage in a model of transient forebrain ischemia.** *Ann Neurol* 1982, **11(5)**:491-498.
3. Smith ML, Auer RN, Siesjo BK: **The density and distribution of ischemic brain injury in the rat following 2-10 min of forebrain ischemia.** *Acta Neuropathol* 1984, **64(4)**:319-332.
4. Hata R, Matsumoto M, Hatakeyama T, Ohtsuki T, Handa N, Niinobe M, Mikoshiba K, Sakaki S, Nishimura T, Yanagihara T, *et al*: **Differential vulnerability in the hindbrain neurons and local cerebral blood flow during bilateral vertebral occlusion in gerbils.** *Neuroscience* 1993, **56(2)**:423-439.
5. Kirino T: **Delayed neuronal death in the gerbil hippocampus following ischemia.** *Brain Res* 1982, **239(1)**:57-69.
6. Kitagawa K, Matsumoto M, Niinobe M, Mikoshiba K, Hata R, Ueda H, Handa N, Fukunaga R, Isaka Y, Kimura K, *et al*: **Microtubule-associated protein 2 as a sensitive marker for cerebral ischemic damage–immunohistochemical investigation of dendritic damage.** *Neuroscience* 1989, **31(2)**:401-411.
7. Reichenberger I, Dieringer N: **Size-related colocalization of glycine and glutamate immunoreactivity in frog and rat vestibular afferents.** *J Comp Neurol* 1994, **349(4)**:603-614.
8. Doi K, Tsumoto T, Matsunaga T: **Actions of excitatory amino acid antagonists on synaptic inputs to the rat medial vestibular nucleus: an electrophysiological study in vitro.** *Exp Brain Res* 1990, **82(2)**:254-262.
9. Popper P, Rodrigo JP, Alvarez JC, Lopez I, Honrubia V: **Expression of the AMPA-selective receptor subunits in the vestibular nuclei of the chinchilla.** *Brain Res Mol Brain Res* 1997, **44(1)**:21-30.
10. Gorter JA, Petrozzino JJ, Aronica EM, Rosenbaum DM, Opitz T, Bennett MV, Connor JA, Zukin RS: **Global ischemia induces downregulation of Glur2 mRNA and increases AMPA receptor-mediated Ca2+ influx in hippocampal CA1 neurons of gerbil.** *J Neurosci* 1997, **17(16)**:6179-6188.
11. Hossmann KA: **Reperfusion of the brain after global ischemia: hemodynamic disturbances.** *Shock* 1997, **8(2)**:95-101.
12. Bodsch W, Takahashi K, Barbier A, Ophoff BG, Hossmann KA: **Cerebral protein synthesis and ischemia.** *Prog Brain Res* 1985, **63**:197-210.
13. Barone FC, Feuerstein GZ: **Inflammatory mediators and stroke: new opportunities for novel therapeutics.** *J Cereb Blood Flow Metab* 1999, **19(8)**:819-834.

14. Siesjo BK, Agardh CD, Bengtsson F: **Free radicals and brain damage.** *Cerebrovasc Brain Metab Rev* 1989, **1(3)**:165-211.
15. Abe K, Aoki M, Kawagoe J, Yoshida T, Hattori A, Kogure K, Itoyama Y: **Ischemic delayed neuronal death. A mitochondrial hypothesis.** *Stroke* 1995, **26(8)**:1478-1489.
16. Du C, Hu R, Csernansky CA, Hsu CY, Choi DW: **Very delayed infarction after mild focal cerebral ischemia: a role for apoptosis?** *J Cereb Blood Flow Metab.* 1996, **16(2)**:195-201.
17. Johnson GV, Jope RS: **The role of microtubule-associated protein 2 (MAP-2) in neuronal growth, plasticity, and degeneration.** *J Neurosci Res* 1992, **33(4)**:505-512.
18. Siman R, Noszek JC: **Excitatory amino acids activate calpain I and induce structural protein breakdown in vivo.** *Neuron* 1988, **1(4)**:279-287.
19. Halpain S, Greengard P: **Activation of NMDA receptors induces rapid dephosphorylation of the cytoskeletal protein MAP2.** *Neuron* 1990, **5(3)**:237-246.
20. Dawson DA, Hallenbeck JM: **Acute focal ischemia-induced alterations in MAP2 immunostaining: description of temporal changes and utilization as a marker for volumetric assessment of acute brain injury.** *J Cereb Blood Flow Metab* 1996, **16(1)**:170-174.
21. Imai Y, Ibata I, Ito D, Ohsawa K, Kohsaka S: **A novel gene iba1 in the major histocompatibility complex class III region encoding an EF hand protein expressed in a monocytic lineage.** *Biochem Biophys Res Commun* 1996, **224(3)**:855-862.
22. Imai Y, Kohsaka S: **Intracellular signaling in M-CSF-induced microglia activation: role of Iba1.** *Glia* 2002, **40(2)**:164-174.
23. Tanaka R, Komine-Kobayashi M, Mochizuki H, Yamada M, Furuya T, Migita M, Shimada T, Mizuno Y, Urabe T: **Migration of enhanced green fluorescent protein expressing bone marrow-derived microglia/macrophage into the mouse brain following permanent focal ischemia.** *Neuroscience* 2003, **117(3)**:531-539.
24. Schilling M, Besselmann M, Leonhard C, Mueller M, Ringelstein EB, Kiefer R: **Microglial activation precedes and predominates over macrophage infiltration in transient focal cerebral ischemia: a study in green fluorescent protein transgenic bone marrow chimeric mice.** *Exp Neurol* 2003, **183(1)**:25-33.
25. Hwang IK, Yoo KY, Kim DW, Choi SY, Kang TC, Kim YS, Won MH: **Ionized calcium-binding adapter molecule 1 immunoreactive cells change in the gerbil hippocampal CA1 region after ischemia/reperfusion.** *Neurochem Res* 2006, **31(7)**:957-965.
26. Denes A, Vidyasagar R, Feng J, Narvainen J, McColl BW, Kauppinen RA, Allan SM: **Proliferating resident microglia after focal cerebral ischaemia in mice.** *J Cereb Blood Flow Metab* 2007, **27(12)**:1941-1953.
27. Cao F, Hata R, Zhu P, Niinobe M, Sakanaka M: **Up-regulation of syntaxin1 in ischemic cortex after permanent focal ischemia in rats.** *Brain Res* 2009, **1272**:52-61.
28. Morioka T, Kalehua AN, Streit WJ: **The microglial reaction in the rat dorsal hippocampus following transient forebrain ischemia.** *J Cereb Blood Flow Metab* 1991, **11(6)**:966-973.
29. Che X, Ye W, Panga L, Wu DC, Yang GY: **Monocyte chemoattractant protein-1 expressed in neurons and astrocytes during focal ischemia in mice.** *Brain Res* 2001, **902(2)**:171-177.
30. Biber K, Sauter A, Brouwer N, Copray SC, Boddeke HW: **Ischemia-induced neuronal expression of the microglia attracting chemokine Secondary Lymphoid-tissue Chemokine (SLC).** *Glia* 2001, **34(2)**:121-133.
31. Wang HK, Park UJ, Kim SY, Lee JH, Kim SU, Gwag BJ, Lee YB: **Free radical production in CA1 neurons induces MIP-1alpha expression, microglia recruitment, and delayed neuronal death after transient forebrain ischemia.** *J Neurosci* 2008, **28(7)**:1721-1727.
32. Furuichi Y, Noto T, Li JY, Oku T, Ishiye M, Moriguchi A, Aramori I, Matsuoka N, Mutoh S, Yanagihara T: **Multiple modes of action of tacrolimus (FK506) for neuroprotective action on ischemic damage after transient focal cerebral ischemia in rats.** *Brain Res* 2004, **1014(1-2)**:120-130.

doi:10.1186/1471-2202-11-115
Cite this article as: Cao *et al.*: Delayed neuronal cell death in brainstem after transient brainstem ischemia in gerbils. *BMC Neuroscience* 2010 11:115.

Neuroscience Letters 473 (2010) 237–241

Contents lists available at ScienceDirect

Neuroscience Letters

journal homepage: www.elsevier.com/locate/neulet

Protective effects of exogenous GM-1 ganglioside on acoustic injury of the mouse cochlea

Shuho Tanaka, Keiji Tabuchi *, Tomofumi Hoshino, Hidekazu Murashita, Shigeki Tsuji, Akira Hara

Department of Otolaryngology, Graduate School of Comprehensive Human Sciences, University of Tsukuba, 1-1-1 Tennodai, Tsukuba 305-8575, Japan

ARTICLE INFO

Article history:
Received 13 January 2010
Received in revised form 16 February 2010
Accepted 22 February 2010

Keywords:
GM-1 ganglioside
Acoustic injury
4-Hydroxynonenal
Lipid peroxidation

ABSTRACT

GM-1 ganglioside (GM-1), a glycosphingolipid, is embedded in the lipid layer of neuronal membranes and is one of the neuroprotective agents. To the best of our knowledge, the role of GM-1 has never been examined in hair cell injury. The purpose of this study was therefore to evaluate the effects of GM-1 on acoustic injury of the cochlea. Mice were exposed to 4-kHz pure tone of 128 dB SPL (sound pressure level) for 4 h. GM-1 was intraperitoneally administered immediately before the onset of acoustic overexposure. The threshold shift of the auditory brainstem response (ABR) and hair cell loss were then evaluated 2 weeks after acoustic overexposure. Immunostaining for 4-hydroxynonenal (4-HNE), indicative of lipid peroxidation, was also examined in animals subjected to acoustic overexposure. GM-1 treatment significantly decreased the ABR threshold shifts and hair cell loss after acoustic overexposure. And immunostaining for 4-HNE was reduced by GM-1 treatment. These findings suggest that GM-1 is involved in the protection of the cochlea against acoustic injury through inhibiting lipid peroxidation.

GM-1 ganglioside (GM-1), a glycosphingolipid with an attached monosialic acid moiety, is found in high concentrations embedded in the external lipid layer of neuronal membranes [29,31]. GM-1 is known to exist in clusters and form microdomains, known as lipid rafts [13,26]. GM-1 is considered to modulate various protein kinase activities [37], Ca^{2+} flux [11] and neurite outgrowth [21]. In addition, GM-1 and other brain gangliosides possess antioxidant activity, significantly reducing the accumulation of lipid peroxide products and free radical production. Because of its neuroprotective and neurorestorative properties, GM-1 ganglioside has been clinically administered such as those with spinal cord injury and Alzheimer's disease [1,2,8,31].

Exposure to high sound pressure levels causes hearing loss by damaging sensory hair cells of the cochlea, e.g., [33]. Many reports have demonstrated that the progression of acoustic injury is advanced by oxidative stress [10,25,35,42]. Endogenous antioxidants such as glutathione [41], superoxide dismutase [16], and alpha-tocopherol [15] protect the inner ear by reducing the generation of free radicals.

The presence of GM-1 in the cochlea has been demonstrated by Santi et al. [23]. We hypothesized that GM-1 protects the cochlea against acoustic injury by reducing free radicals. In this study, we examined the effects of GM-1 ganglioside on acoustic injury of the cochlea.

Seventy-six female ddY mice, 8 weeks of age, were purchased from Japan SLC (Hamamatsu, Japan). The ddY mouse is frequently used as a subject for pharmacological and toxicological experiments in Japan. The care and use of animals was approved by the Animal Experiment Committee of the University of Tsukuba.

Mice were anesthetized with an intraperitoneal injection of pentobarbital sodium (50 mg/kg body weight). Positive, negative, and ground electrodes were inserted subcutaneously at the vertex, mastoid, and back, respectively. Bursts of pure tone (rise and fall times; 1 ms, duration; 10 ms, repetition rate; 20/s in an open field system) were used to evoke the ABR. Evoked responses were filtered with a band pass of 200–3000 Hz and averaged over 1000 sweeps using a signal processor (Synax 1200, NEC, Tokyo, Japan). The sound intensity varied in 5-dB steps. The ABR was measured at three frequencies (4, 8, and 16 kHz) before, immediately after and 2 weeks after acoustic overexposure. ABR threshold shifts from pre-exposure levels were then examined 2 weeks after acoustic overexposure.

The mice were exposed to a 4-kHz pure tone of 128 dB SPL for 4 h through an open field system inside a sound-exposure chamber (Type 4212, Brüel & Kjaer, Copenhagen, Denmark), in which two small cages (4 cm × 3 cm × 6 cm) were placed [17,36]. Two mice were subjected at the same time.

The mice were sacrificed under deep anesthesia 2 weeks after acoustic overexposure. Cardiac perfusion was performed with 4% paraformaldehyde in 0.1 M phosphate-buffered saline. Cochleae were quickly removed, immersed in the same fixative at 4 °C for 8 h, and then decalcified with ethylenediaminetetraacetic acid for

* Corresponding author. Tel.: +81 29 853 3147; fax: +81 29 853 3147.
E-mail address: ktabuchi@md.tsukuba.ac.jp (K. Tabuchi).

0304-3940/$ – see front matter © 2010 Elsevier Ireland Ltd. All rights reserved.
doi:10.1016/j.neulet.2010.02.057

1 week. After decalcification, cochleae were dissected as surface preparations, and the nuclei of hair cells were stained with propidium iodide (PI, 2 μg/ml in PBS, Molecular Probes Inc., OR, U.S.A.) in darkness.

The number of missing hair cells (absence of PI staining) was counted under a laser confocal microscope (TCS SP2, Leica Microsystems, Wetzlar, Germany) around the 66% region from the apex of the cochlea. Our previous reports clarified that acoustic overexposure to 128 dB SPL for 4 h of mice induced hearing loss and the maximum hair cell loss at the 66% region from the apex of the cochlea [17,36].

Immunocytochemical analyses were carried out on cryostat sections. The methods for the fixation and decalcification of cochleae were the same as those described in the above section. Cryostat sections were then made parallel to the modiolus to identify the organ of Corti on microscope slides. The cryostat sections of 6 μm were incubated in 0.5% Triton X-100 and blocked in calf serum for 10 min at room temperature. The sections were then washed with PBS, followed by incubation with the primary antibody at a concentration of 1:100 (anti-4HNE) (Abcam, MA, U.S.A.) at 4 °C for 72 h. The sections were then incubated with the secondary antibody at a concentration of 1:200 (anti-goat IgG conjugated with FITC) (Abcam, MA, U.S.A.) and with PI (2 μg/ml in PBS) at room temperature for 30 min in darkness. Immunolabeling was visualized using a laser microscope (BX51-DP71-SET, OLYMPUS, Tokyo, Japan). Control incubations were routinely processed without primary antibody. The density level of immunofluorolabeling of three outer hair cells was assessed in each cochlea with the freely available image analysis software program ImageJ (National Institutes of Health, Bethesda, MD, U.S.A.).

GM-1 was purchased from Wako (Japan), and dissolved in physiological saline solution. GM-1 and saline were administered immediately before the onset of acoustic overexposure. Mice were randomly assigned to one of the following 4 treatment groups:

(1) 1 mg/kg GM-1-treated group ($n = 6$)
(2) 10 mg/kg GM-1-treated group ($n = 6$)
(3) 30 mg/kg GM-1-treated group ($n = 6$)
(4) noise-alone group ($n = 6$).

Immunostaining for 4-HNE before acoustic overexposure without any drugs ($n = 4$) was examined. And immunostaining for 4-HNE of the noise-alone group ($n = 4$) and the GM-1 (30 mg/kg) treatment group ($n = 4$) were compared at each following time points: 0 h, 4 h, 12 h, 1 day, 3 days and 7 days after acoustic overexposure.

All data are expressed as the mean ± S.D. The comparison of ABR threshold shifts or hair cell loss between each group was performed by one-way and two-way analysis of variance (ANOVA), and then the Scheffé test and Fisher's PLSD test were used. Comparison of the densitometry on immunofluorolabeling with 4-HNE was performed using Student's t-test. A p-value of less than 0.05 was considered significant.

Fig. 1 demonstrates ABR threshold shifts 2 weeks after acoustic overexposure, respectively. The GM-1 (1 mg/kg) and GM-1 (10 mg/kg) groups did not significantly reduce ABR threshold shifts (two-way ANOVA, Scheffé test and Fisher's PLSD test, $p > 0.05$). On the other hand, the GM-1 (30 mg/kg) group showed a significantly decreased ABR threshold shift (two-way ANOVA, Scheffé test and Fisher's PLSD test, $p < 0.01$).

Fig. 2 demonstrates representative photographs of hair cell loss at the 66% region from the apex of the cochlea in the noise-alone and GM-1 (30 mg/kg) groups. The quantitative analysis of hair cell loss is shown in Fig. 3. As expected from the ABR studies, 30 mg/kg GM-1 significantly ameliorated outer hair cell loss, especially in the first row, as compared with the noise-alone group (two-way ANOVA; $p < 0.05$, one-way ANOVA; $p < 0.05$ in the first row, Fig. 3).

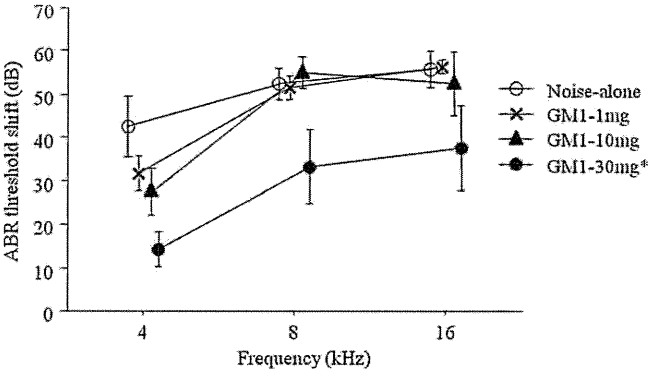

Fig. 1. ABR threshold shifts 2 weeks after acoustic overexposure. GM-1 ganglioside significantly decreased ABR threshold shifts 2 weeks after acoustic overexposure at only 30 mg/kg (two-way ANOVA and Scheffé test: $^*p < 0.05$).

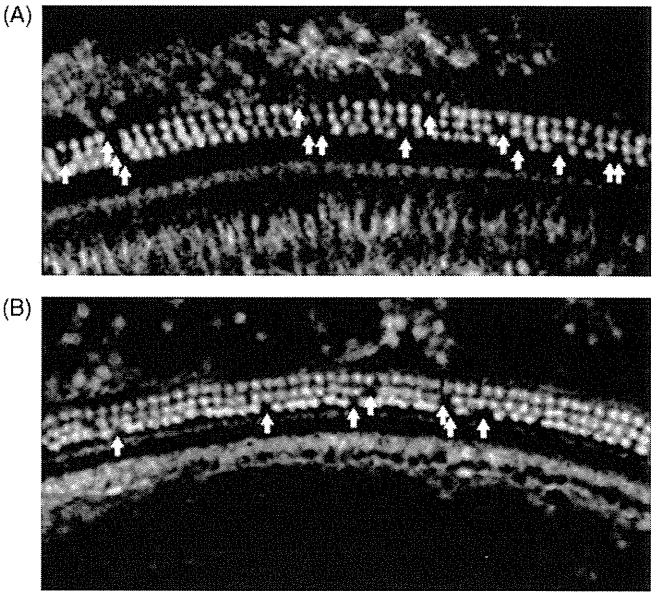

Fig. 2. (A) Representative microscopic fluorescence image of hair cell nuclei in the noise-alone group 2 weeks after acoustic overexposure. (B) Representative image of the 30 mg/kg GM-1 ganglioside group. Arrows indicate hair cell loss. The 30 mg/kg GM-1 ganglioside group was less hair cell loss than noise-alone group.

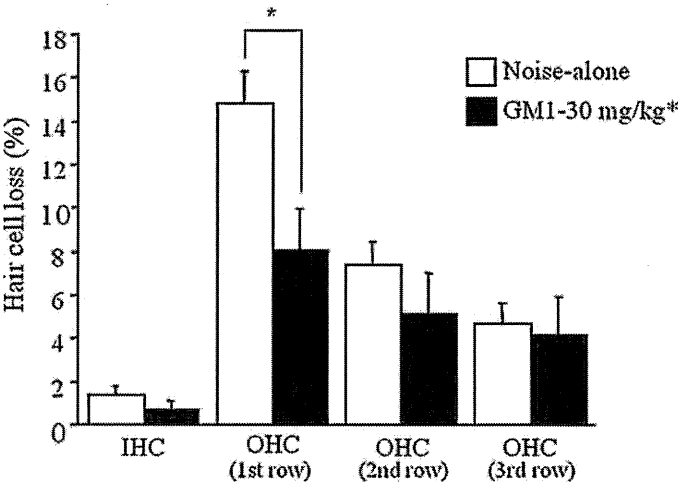

Fig. 3. The effect of 30 mg/kg GM-1 ganglioside on hair cell loss after acoustic overexposure. Missing hair cells at the 66% region from the apex were calculated 2 weeks after acoustic overexposure. Treatment with GM-1 significantly decreased loss of OHCs, especially in the first row (two-way ANOVA: $^*p < 0.05$, one-way ANOVA: $^*p < 0.05$ in the first row). IHC: inner hair cell, OHC1: the first row of outer hair cells, OHC2: the second row of outer hair cells, OHC3: the third row of outer hair cells.

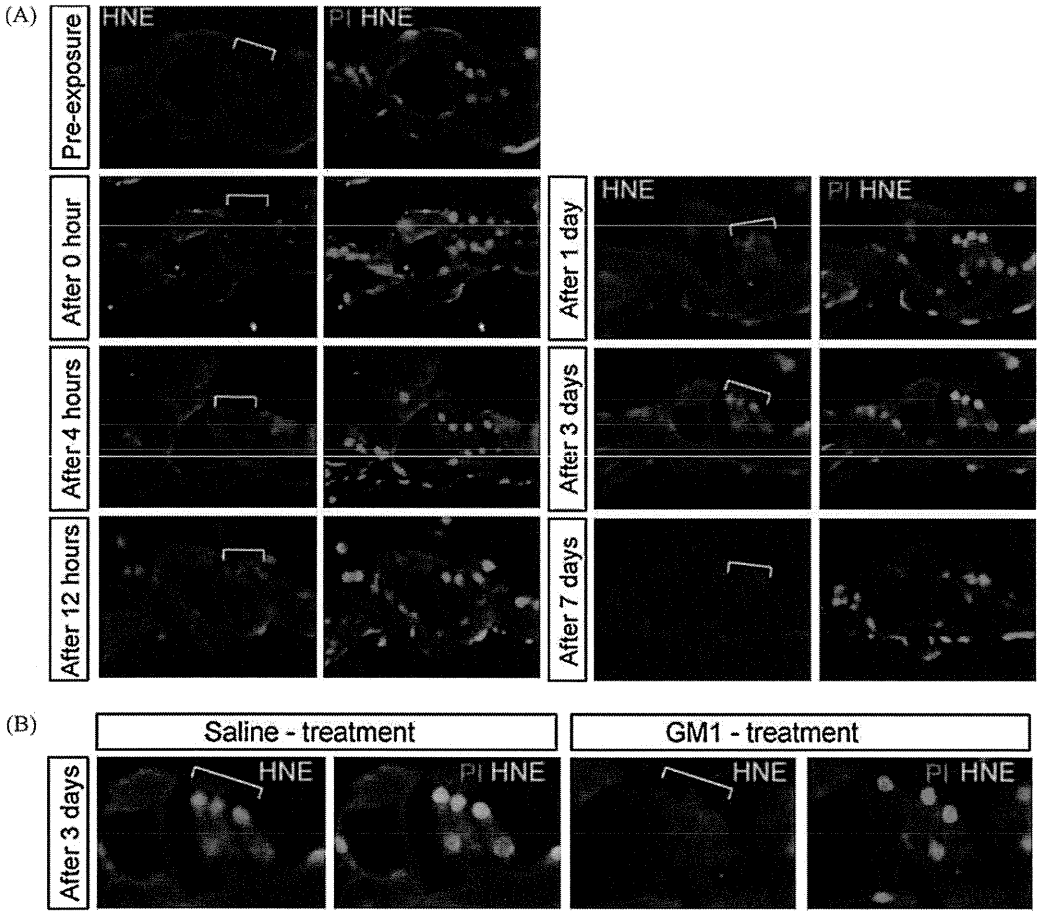

Fig. 4. Representative photographs of 4-HNE immunostaining of the organ of Corti. (A) Photographs of the noise-alone group before and after overexposure. (B) Representative images 3 days after acoustic overexposure of the noise-alone and GM-1 (30 mg/kg) groups.

4-HNE was broadly stained in the sensory epithelium (organ of Corti) of both groups at all time points (Fig. 4A). Slight staining was observed even before acoustic overexposure (Fig. 4A). In the noise-alone group, staining with 4-HNE gradually increased until 12 h after acoustic overexposure, and staining was clearly observed at 12 h to 3 days after. The staining then became weak at 7 days after (Fig. 4A). The time-course of 4-HNE staining in the GM-1 (30 mg/kg) group was essentially similar to that of the noise-alone group. The highest density was seen at 12 h to 3 days after (Fig. 4B). On the other hand, when comparing the staining at each time point, there was tendency for staining in the GM-1 (30 mg/kg) group to be weaker than that of the noise-alone group (Fig. 5). Fig. 5 shows the relative densities of 4-HNE staining in the outer hair cells subtracted from the pre-exposure level. Staining differences between both groups reached significance from 4 h to 3 days ($n = 5$ at each time point, Student's t-test: $^*p < 0.05$) (Fig. 5). However, the difference in density was not clear at 7 days (Fig. 4A).

GM-1 administered before acoustic overexposure significantly decreased ABR threshold shifts and hair cell loss at 2 weeks after acoustic overexposure. The present findings clearly demonstrated that GM-1 ganglioside ameliorated the permanent threshold shifts induced by acoustic overexposure. To our knowledge, this is the first report that GM-1 ganglioside has protective effects on hair cells against cochlear injury. Previous studies have shown the protective effect of GM-1 on the spiral ganglion and cochlear nucleus [20,38].

It has been demonstrated that acoustic injury damages the cochlea by producing free radicals. Many reports have demonstrated that antioxidants and free radical scavengers exhibit protective effects against acoustic injury, e.g., glutathione [41], superoxide dismutase [16], methylprednisolone [32,34], vitamin A, C, or E [15], and tempol [17]. Acoustic overexposure initially damages the outer hair cells, and these agents effectively prevented the injury of outer hair cells. Our study is consistent with these previous studies.

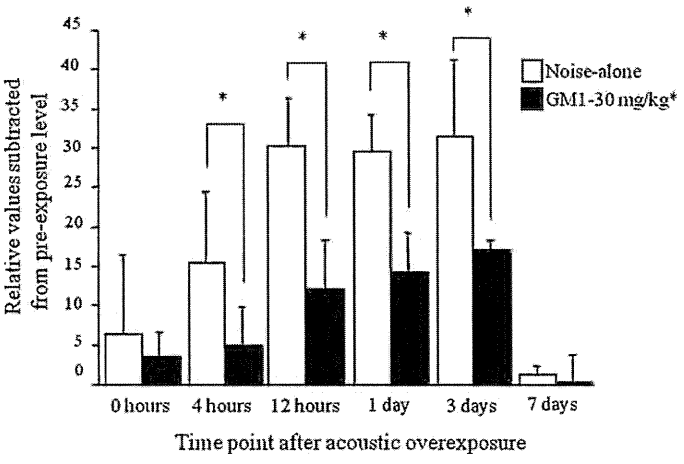

Fig. 5. Densities of 4-HNE in the outer hair cells. Relative values subtracted from the pre-exposure level are shown. The time-course of the immunostaining density in the GM-1 (30 mg/kg) group was similar to that of the noise-alone group. The highest density was seen at 12 h to 3 days after overexposure. Each density of immunostaining in the GM-1 (30 mg/kg) group was significantly weaker than that of the noise-alone group at the same time points from 4 h to 3 days ($n = 5$ at each time point, Student's t-test: $^*p < 0.05$).

In this study, we evaluated the staining of 4-HNE in the organ of Corti. 4-HNE is a toxic aldehyde commonly used as an indicator of lipid peroxidation. Oxidative stress within a cell generates reactive oxygen species that interact with phospholipids in the cell membrane to cause their peroxidation [9]. 4-HNE is produced in the cochlea damaged by sound-induced trauma, and has been shown to cause the apoptosis of auditory neurons in vitro [24,40]. Triamcinolone acetonide and glutathione were two agents shown to protect hair cells from hydroxynonenal-induced cell death [9,22]. GM-1 treatment decreased 4-HNE staining of outer hair cells in this study. This finding indicated that GM-1 protected outer hair cells through inhibiting the toxic effects of free radicals and hydroxynonenals.

GM-1 was reported to have the neuroprotective effect on the cytotoxic action of hydrogen peroxide in PC12 cells which were sensitive to oxidative stress [29,43]. GM-1 prevented the accumulation of malondialdehyde (MDA), a marker of oxidative stress, and the inactivation of Na^+-K^+-ATPase induced by hydrogen peroxide in PC12 cells. GM-1 prevented the oxidative inactivation of Na^+-K^+-ATPase induced by glutaric acid and pentylenetetrazole [7]. GM-1 was reported to decrease the glutamate-induced activation of free radical reactions in nerve cells, and also reduced neuronal death in a rat cerebellar granule cell culture [3,4]. These studies also revealed the antioxidant properties of ganglioside, and thus supported our present findings.

GM-1 is abundantly embedded in the lipid layer of neuronal membranes. Recent studies suggest that GM-1 can function as a primary lipid messenger on the cell membrane responding to marked stress. GM-1 is inserted into the plasma membrane as the hydrophobic ceramide portion of the molecule becomes embedded in the outer leaflet of the plasma membrane and its carbohydrate portion extends into the extracellular space [28]. This ceramide portion forms a domain receiving many external signals. Many biochemical studies reported that domains transmitted signals from the extracellular space to cytosol. These lipid rafts are associated with a variety of signaling molecules, such as GPI-anchored proteins [19], non-receptor and receptor tyrosine kinases [39], Src-family tyrosine kinases [12], and trimeric GTP-binding proteins [5] on the inside of the cell membrane. They may control mitogen-activated protein kinase (MAPK) activities, S6 kinase activities [37], the phosphorylation of Trk [18], and Ca^{2+} flux [11]. Thus, GM-1 may be a kind of potentiator or modulator of trophic factors in both the peripheral and central nervous systems [6,14,27,28,30]. Further studies are necessary to clarify the involvement of the protective mechanisms of GM-1 other than its antioxidative property.

In conclusion, we showed herein that GM-1 is able to protect the cochlea against acoustic injury. The immunocytochemistry of hair cells revealed that the antioxidant property of GM-1 was important for the protection.

Acknowledgements

This work was supported by Grants-in-aid for Scientific Research (C)20591969 and (C)20591970 from the Ministry of Education, Culture, Sports, Science, and Technology of Japan.

References

[1] M. Alter, GM1 ganglioside for acute ischemic stroke, trial design issues, Ann. N.Y. Acad. Sci. 845 (1998) 391–401.
[2] C. Argentino, M.L. Sacchetti, D. Toni, G. Savoini, E. D'Arcangelo, F. Erminio, F. Federico, F.F. Milone, V. Gallai, D. Gambi, GM1 ganglioside therapy in acute ischemic stroke. Italian acute stroke study-hemodilution+drug, Stroke 20 (1989) 1143–1149.
[3] N.F. Avrova, I.V. Victorov, V.A. Tyurin, I.O. Zakharova, T.V. Sokolova, N.A. Andreeva, E.V. Stelmaschuk, Y.Y. Tyurina, V.S. Gonchar, Inhibition of glutamate-induced intensification of free radical reactions by gangliosides: possible role in their protective effect in rat cerebellar granule cells and brain synaptosomes, Neurochem. Res. 23 (1998) 945–952.
[4] N.F. Avrova, K.I. Shestak, I.O. Zakharova, T.V. Sokolova, Y.Y. Tyurina, V.A. Tyurin, The use of antioxidants to prevent glutamate-induced derangement of calcium ion metabolism in rat cerebral cortex synaptosomes, Neurosci. Behav. Physiol. 30 (2000) 535–541.
[5] P.L. Cameron, J.W. Ruffin, R. Bollag, H. Rasmussen, R.S. Cameron, Identification of caveolin and caveolin-related proteins in the brain, J. Neurosci. 17 (1997) 9520–9535.
[6] P. Doherty, J.G. Dickson, T.P. Flanigan, F.S. Walsh, Ganglioside GM1 does not initiate, but enhances neurite regeneration of nerve growth factor-dependent sensory neurons, J. Neurochem. 44 (1985) 1259–1265.
[7] M.R. Fighera, L.F. Royes, A.F. Furian, M.S. Oliveira, N.G. Fiorenza, R. Frussa-Filho, J.C. Petry, R.C. Coelho, C.F. Mello, GM1 ganglioside prevents seizures, Na^+,K^+-ATPase activity inhibition and oxidative stress induced by glutaric acid and pentylenetetrazole, Neurobiol. Dis. 22 (2006) 611–623.
[8] F.H. Geisler, F.C. Dorsey, W.P. Coleman, Past and current clinical studies with GM-1 ganglioside in acute spinal cord injury, Ann. Emerg. Med. 22 (1993) 1041–1047.
[9] J. Guzman, J. Ruiz, A.A. Eshraghi, M. Polak, C. Garnham, T.J. Balkany, T.R. Van De Water, Triamcinolone acetonide protects auditory hair cells from 4-hydroxy-2,3-nonenal (4-HNE) ototoxicity in vitro, Acta Otolaringol. 126 (2006) 685–690.
[10] A. Hara, F. Serizawa, K. Tabuchi, M. Senarita, J. Kusakari, Hydroxyl radical formation in the perilymph of asphyxic guinea pig, Hear. Res. 143 (2000) 110–114.
[11] B.S. Hilbush, J.M. Levine, Modulation of a Ca^{2+} signaling pathway by GM1 ganglioside in PC12 cells, J. Biol. Chem. 267 (1992) 24789–24795.
[12] K. Kasahara, Y. Watanabe, T. Yamamoto, Y. Sanai, Association of Src family tyrosine kinase Lyn with ganglioside GD3 in rat brain. Possible regulation of Lyn by glycosphingolipid in caveolae-like domains, J. Biol. Chem. 277 (1997) 29947.
[13] R.W. Ledeen, Ganglioside structures and distribution: are they localized at the nerve ending? J. Supramol. Struct. 8 (1978) 1–17.
[14] A. Leon, D. Benvegnu, R. Dal Toso, D. Presti, L. Facci, O. Giorgi, G. Toffano, Dorsal root ganglia and nerve growth factor: a model for understanding the mechanism of GM1 effects on neuronal repair, J. Neurosci. Res. 12 (1984) 277–287.
[15] C.G. Le Prell, L.F. Hughes, J.M. Miller, Free radical scavengers vitamins A, C, and E plus magnesium reduce noise trauma, Free Radic. Biol. Med. 42 (2007) 1454–1463.
[16] S.L. McFadden, K.K. Ohlemiller, D. Ding, M. Shero, R.J. Salvi, The influence of superoxide dismutase and glutathione peroxidase deficiencies on noise-induced hearing loss in mice, Noise Health 3 (2001) 49–64.
[17] H. Murashita, K. Tabudhi, T. Hoshino, S. Tsuji, A. Hara, The effects of tempol, 3-aminobenzamide and nitric oxide synthase inhibitors on acoustic injury of the mouse cochlea, Hear. Res. 214 (2006) 1–6.
[18] T. Mutoh, A. Tokuda, T. Miyadai, M. Hamaguchi, N. Fujiki, Ganglioside GM1 binds to the Trk protein and regulates receptor function, Proc. Natl. Acad. Sci. U.S.A. 92 (1995) 5087–5091.
[19] S. Olive, C. Dubois, M. Schachner, G. Rougon, The F3 neuronal glycosylphosphatidylinositol-linked molecule is localized to glycolipid-enriched membrane subdomains and interacts with L1 and fyn kinase in cerebellum, J. Neurochem. 65 (1995) 2307–2317.
[20] C.W. Parkins, L. Li, D.W. Webster, Comparison of GM1 ganglioside treatment and electrical stimulation for preventing spiral ganglion cell loss in pharmacologically deafened guinea pig, Assoc. Res. Otolaringol. Abs. 22 (1999) 167.
[21] F.J. Roisen, H. Bartfeld, R. Nagele, G. Yorke, Ganglioside stimulation of axonal sprouting in vitro, Science 214 (1981) 577–578.
[22] J.W. Ruiz, J. Guzman, M. Polak, A.A. Eshraghi, T.J. Balkany, T.R. Van De Water, Glutathione ester protects against hydroxynonenal-induced loss of auditory hair cells, Otolaryngol. Head Neck Surg. 135 (2006) 792–797.
[23] P.A. Santi, P. Mancini, C. Barnes, Identification and localization of the GM1 ganglioside in the cochlea using thin-layer chromatography and cholera toxin, J. Histochem. Cytochem. 42 (1994) 705–716.
[24] U. Scarpidis, D. Madnani, C. Shoemaker, C.H. Fletcher, K. Kojima, A.A. Eshraghi, Arrest of apoptosis in auditory neurons: implications for sensorineural preservation in cochlear implantation, Otol. Neurotol. 24 (2003) 409–417.
[25] M.D. Seidman, B.G. Shivapuja, W.S. Quirk, The protective effects of allopurinol and superoxide dismutase on noise-induced cochlear damage, Otolaryngol. Head Neck Surg. 109 (1993) 1052–1056.
[26] K. Simons, D. Toomre, Lipid rafts and signal transduction, Nat. Rev. Mol. Cell Boil. 1 (2000) 31–39.
[27] S.D. Skaper, R. Katoh-Semba, S. Varon, GM1 ganglioside accelerates neurite outgrowth from primary peripheral and central neurons under selected culture conditions, Dev. Brain Res. 23 (1985) 19–26.
[28] S.D. Skaper, A. Leon, G. Toffano, Ganglioside function in the development and repair of the nervous system, Mol. Neurobiol. 3 (1989) 173–199.
[29] T.V. Sokolova, I.O. Zakharova, V.V. Furaev, M.P. Rychkova, N.F. Avrova, Neuroprotective effect of ganglioside GM1 on the cytotoxic action of hydrogen peroxide and amyloid beta-peptide in PC12 cells, Neurochem. Res. 32 (2007) 1302–1313.
[30] P.E. Spoerri, F.J. Roisen, Ganglioside potentiation of NGF-independent trophic agents on sensory ganglia, Neurosci. Lett. 90 (1988) 21–26.
[31] L. Svennerholm, Ganglioside—a new therapeutic agent against stroke and Alzheimer's disease, Life Sci. 55 (1994) 2125–2134.
[32] K. Tabuchi, H. Murashita, S. Sakai, T. Hoshino, I. Uemaetomari, A. Hara, Therapeutic time window of methylprednisolone in acoustic injury, Otol. Neurotol. 27 (2006) 1176–1179.

[33] K. Tabuchi, H. Murashita, A. Hara, Acoustic injury of the cochlea: the role of reactive oxygen species and mechanisms of hair cell death, in: Recent Advances in Auditory neuroscience, Research Signpost, Kerala, India, 2007, pp. 11–18.
[34] K. Takahashi, J. Kusakari, S. Kimura, T. Wada, A. Hara, The effect of methylprednisolone on acoustic trauma, Acta Otolaryngol. 116 (1996) 209–212.
[35] T. Takemoto, K. Sugawara, T. Okuda, H. Shimogori, H. Yamashita, The clinical free radical scavenger, edaravone, protects cochlear hair cells from acoustic trauma, Eur. J. Pharmacol. 487 (2004) 113–116.
[36] I. Uemaetomari, K. Tabuchi, T. Hoshino, A. Hara, Protective effect of calcineurin inhibitors on acoustic injury of the cochlea, Hear. Res. 209 (2005) 86–90.
[37] J.R. Van Brocklyn, J.R. Vandenheede, R. Fertel, A.J. Yates, A.A. Rampersaud, Ganglioside, GM1 activates the mitogen-activated protein kinase Erk2 and p70 S6 kinase in U-1242 MG human glioma cells, J. Neurochem. 69 (1997) 116.
[38] M.E. Walsh, D.B. Webster, Exogenous GM1 ganglioside effects on conductive and sensorineural hearing losses, Hear. Res. 75 (1994) 54–60.
[39] C. Wu, S. Butz, Y. Ying, R.G. Anderson, Tyrosine kinase receptors concentrated in caveolae-like domains from neuronal plasma membrane, J. Biol. Chem. 272 (1997) 3554–3559.
[40] D. Yamashita, H.-Y. Jiang, J. Schacht, J.M. Miller, Delayed production of free radicals following noise exposure, Brain Res. 1019 (2004) 201–209.
[41] T. Yamasoba, A.L. Nuttall, C. Harris, Y. Raphael, J.M. Miller, Role of gluthathione in protection against noise-induced hearing loss, Brain Res. 784 (1998) 82–90.
[42] T. Yamasoba, J. Schacht, F. Shoji, J.M. Miller, Attenuation of cochlear damage from noise trauma by an iron chelator, a free radical scavenger and glial cell line-derived neurotrophic factor in vivo, Brain Res. 815 (1999) 317–325.
[43] I.O Zakharova, T.V. Sokolova, V.V. Furaev, M.P. Rychkova, N.F. Avrova, Effects of oxidative stress inducers, neurotoxins, and ganglioside GM1 on Na^+, K^+-ATPase in PC12 and brain synaptosomes, Zh. Evol. Biokhim. Fiziol. 43 (2007) 148–154.

c-Ret–mediated hearing loss in mice with Hirschsprung disease

Nobutaka Ohgami[a], Michiru Ida-Eto[a], Takashi Shimotake[b], Naomi Sakashita[c], Michihiko Sone[d], Tsutomu Nakashima[d], Keiji Tabuchi[e], Tomofumi Hoshino[e], Atsuyoshi Shimada[f], Toyonori Tsuzuki[g], Masahiko Yamamoto[h], Gen Sobue[i], Mayumi Jijiwa[j], Naoya Asai[j], Akira Hara[e], Masahide Takahashi[j], and Masashi Kato[a,1]

[a]Unit of Environmental Health Sciences, Department of Biomedical Sciences, College of Life and Health Sciences, Chubu University, 1200 Matsumoto, Kasugai, Aichi 487-8501, Japan; [b]Department of Pediatric Surgery, Ishikawa Prefectural Central Hospital, Kanazawa, 920-8530, Japan; [c]Department of Pathology, Kumamoto University School of Medicine, Kumamoto, 860-8556, Japan; Departments of [d]Otorhinolaryngology, [i]Neurology, and [j]Pathology, Nagoya University Graduate School of Medicine, Nagoya, 466-8550, Japan; [e]Department of Otolaryngology, Institute of Clinical Medicine, University of Tsukuba, Tsukuba, 305-8575, Japan; [f]Department of Pathology, Institute for Developmental Research, Aichi Human Service Center, Aichi, 480-0392, Japan; [g]Department of Pathology, Nagoya Daini Red Cross Hospital, Nagoya, 466-8650, Japan; and [h]Department of Speech Pathology and Audiology, Aichi Gakuin University School of Health Science, Nisshin, Aichi, 470-0195, Japan

Edited by Jonathan G. Seidman, Harvard Medical School, Boston, MA, and approved June 3, 2010 (received for review April 3, 2010)

A significantly increased risk for dominant sensorineural deafness in patients who have Hirschsprung disease (HSCR) caused by *endothelin receptor type B* and *SOX10* has been reported. Despite the fact that c-*RET* is the most frequent causal gene of HSCR, it has not been determined whether impairments of c-*Ret* and c-*RET* cause congenital deafness in mice and humans. Here, we show that impaired phosphorylation of c-Ret at tyrosine 1062 causes HSCR-linked syndromic congenital deafness in c-*Ret* knockin (KI) mice. The deafness involves neurodegeneration of spiral ganglion neurons (SGNs) with not only impaired phosphorylation of Akt and NF-κB but decreased expression of calbindin D28k in inner ears. The congenital deafness involving neurodegeneration of SGNs in c-*Ret* KI mice was rescued by introducing constitutively activated RET. Taken together with our results for three patients with congenital deafness with c-*RET*–mediated severe HSCR, our results indicate that c-*Ret* and c-*RET* are a deafness-related molecule in mice and humans.

spiral ganglion neuron | syndromic congenital deafness | tyrosine kinase

About 30% of the 120 million people worldwide who suffer from congenital (early-onset) hearing loss are syndromic, and the remaining 70% are nonsyndromic (1–3). To elucidate the etiologies for the hearing losses, inner ears have been morphologically investigated as one of the target tissues. The inner ears contain the organ of Corti and the stria vascularis. The stria vascularis serves to maintain the endolymph potential. The organ of Corti, which consists of two kinds of sensory cells (inner hair cells and outer hair cells) is responsible for mechanotransduction, by which sound impulses are converted into neural impulses. Auditory information from the sensory cells is transmitted to spiral ganglion neurons (SGNs) as the primary carrier, followed by eventual transmission to the auditory cortex (1, 2). Most of the recent studies on hearing have focused on the expression level of a target molecule rather than activities in inner ears (1, 2). Thus, there have been very few studies aimed at determining whether activities of a target molecule cause hearing losses.

The c-*RET* protooncogene encodes a receptor tyrosine kinase, and glial cell-derived neurotrophic factor (GDNF) is one of the ligands for c-RET (4). The GDNF exerts its effect on target cells by binding to a GPI-anchored cell surface protein (GFRα1), which, in turn, recruits the receptor tyrosine kinase c-RET to form a multiple-subunit signaling complex. Formation of this complex results in c-RET autophosphorylation and a cascade of intracellular signaling to control cell survival (4–7).

Tyrosine 1062 (Y1062) in c-Ret is one of the most important autophosphorylation sites for its kinase activation and is a multidocking site for several signaling molecules, including SHC, a transmitter for c-Ret signaling (8–10). c-*RET* has been shown to be essential for the development and maintenance of the enteric nervous system (ENS) in both mice and humans (8, 9) and to be the most frequent causal gene of Hirschsprung disease (HSCR) in humans (20–25% of cases) (11, 12). In fact, severe HSCR with total intestinal aganglionosis has been shown to develop in homozygous knockin (KI) mice, in which Y1062 in c-Ret was replaced with phenylalanine (c-Ret-KI$^{Y1062F/Y1062F}$ mice) (6).

HSCR, which affects 1 in 5,000 births, is a congenital disorder of the ENS, and most cases are thought to be multigenic and multifactorial. A significantly increased risk for dominant sensorineural deafness in patients who have HSCR caused by *endothelin receptor type B* (*EDNRB*) (13) and *SOX10* (14) has been reported (11, 12). Despite the fact that c-*RET* is one of the responsible genes for HSCR, there is no direct evidence to link c-*Ret* and c-*RET* with deafness in mice and humans, presumably because of the short life span [postnatal day (P) 1–2)] of c-*Ret* homozygously deleted mice (15) to measure hearing levels.

In this study, we used c-Ret-KI$^{Y1062F/Y1062F}$ mice, which survive for 3–4 wk, and we focused on whether phosphorylation of c-Ret is relevant to hearing levels. Our results demonstrated that impairment of c-Ret phosphorylation causes syndromic congenital hearing loss with neurodegeneration of SGNs in c-Ret-KI$^{Y1062F/Y1062F}$ mice.

Results

Phosphorylation of c-Ret Y1062 in SGNs Increases in the Process of Hearing Development. We first examined the numbers of c-Ret protein expressed and Y1062-phosphorylated cells in inner ears from WT mice during the developmental stage of hearing after birth (Fig. 1). We found that c-Ret protein and phosphorylated Y1062 were clearly detectable in SGNs from WT mice on P14 (Fig. 1*A* and *B*, arrows). c-Ret protein was constantly expressed in SGNs throughout the hearing developmental stage after birth (P1–18) (Fig. 1*C*, *Left*), whereas the number of Y1062-phosphorylated SGNs was greatly increased in SGNs around P6–7, several days before the WT mice acquire intact hearing levels (around P12) [Fig. 1 *C Right* and *D*). Other areas (e.g., inner and outer hair cells, stria vascularis) of inner ears showed phosphorylated Y1062 in c-Ret (Fig. 1 *A* and *B*, arrowheads), but morphological abnormalities in inner and outer hair cells and the stria vascularis in c-Ret KI$^{Y1062F/Y1062F}$ mice were hardly detected (Figs. S1 and S2). SGNs have been reported to play an essential role in hearing by transmitting auditory information from sensory cells of the cochlea

Author contributions: N.O. and M.K. designed research; N.O., M.I.-E., T.S., and N.S. performed research; M.S., T.N., K.T., T.H., M.Y., G.S., M.J., N.A., A.H., and M.T. contributed new reagents/analytic tools; N.O., T.S., N.S., A.S., T.T., M.T., and M.K. analyzed data; and N.O. and M.K. wrote the paper.

The authors declare no conflict of interest.

This article is a PNAS Direct Submission.

[1]To whom correspondence should be addressed. E-mail: katomasa@isc.chubu.ac.jp.

This article contains supporting information online at www.pnas.org/lookup/suppl/doi:10.1073/pnas.1004520107/-/DCSupplemental.

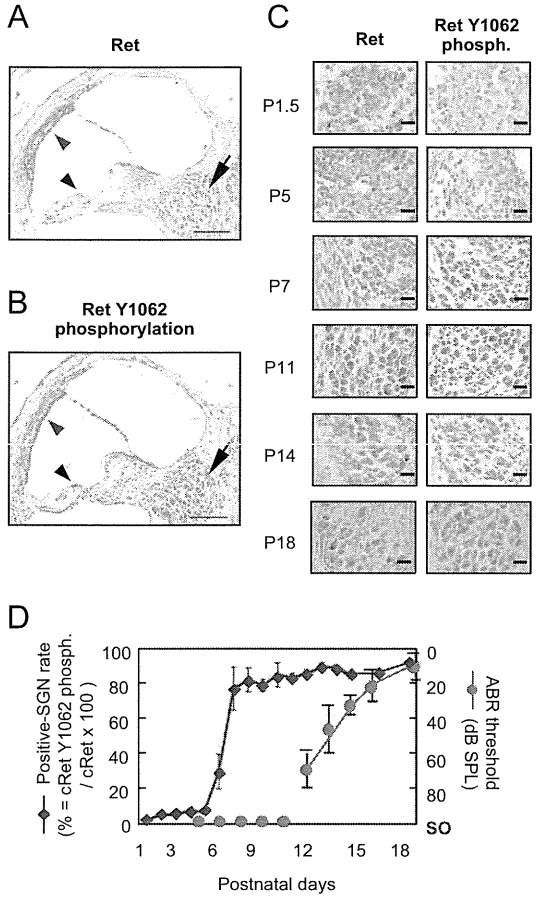

Fig. 1. Increased c-Ret Y1062-phosphorylated SGNs in the process of hearing development in WT mice. Immunohistochemical analyses of c-Ret protein–expressing cells (*A*) and Y1062-phosphorylated cells (*B*) in inner ears from 14-d-old WT mice (C57BL/6). c-Ret protein–expressing (*A*) and Y1062-phosphorylated (*B*) cells were detected in SGNs, acoustic neurons, and the stria vascularis in the inner ear from WT mice. Arrows in *A* and *B* indicate SGNs. Black arrowhead and blue arrowhead in *A* and *B* indicate inner and outer hair cells and stria vascularis, respectively. (*C*) Immunohistochemical analyses for serial sections of c-Ret–expressing (*Left*) and Y1062-phosphorylated (phosph., *Right*) SGNs from WT mice until P18. (Scale bars: *A* and *B*, 100 μm; *C*, 20 μm.) (*D*) Percentage (mean ± SE) of Y1062-phosphorylated SGNs from WT mice during the process of hearing development after birth. The *x* axis indicates days after birth of WT mice. The *y* axis for the blue line (mean ± SE; $n = 3$) indicates the percentage of Y1062-phosphorylated SGNs. The *y* axis for the red line (mean ± SE; $n = 5$) indicates hearing levels of WT mice measured by ABR. The effective measurement range of the ABR system is up to 90- to 100-dB SPL. Scale out (SO) indicates no ABR responses for 90- to 100-dB SPL. The method for staining and estimating the percentage is described in detail in *Materials and Methods*.

to the central nervous system (16). Therefore, we focused on the physiological roles in hearing level of phosphorylation of Y1062 in c-Ret tyrosine kinase in SGNs.

Congenital Deafness in c-Ret-KI$^{Y1062F/Y1062F}$ Mice. We next investigated tone burst-evoked auditory brainstem response (ABR) in c-Ret-KI$^{Y1062F/Y1062F}$ mice (6) to determine whether completely impaired phosphorylation of Y1062 in c-Ret kinase affects hearing levels. Thresholds for sound at 4–40 kHz in 18-d-old c-Ret-KI$^{Y1062F/Y1062F}$ mice [78- to 85-dB sound pressure level (SPL)] were much higher than those in littermate WT mice (20- to 55-dB SPL) (Fig. 2*A*). Latencies of all four ABR waves in c-Ret-KI$^{Y1062F/Y1062F}$ mice were also prolonged (Fig. 2*B*). These results suggest that c-Ret-KI$^{Y1062F/Y1062F}$ mice suffer from severe congenital deafness. On the other hand, hearing levels in other KI mice, in which serine 697 (S697, a putative protein kinase A phosphorylation site) in c-Ret was replaced with alanine (c-Ret-KI$^{S697A/S697A}$ mice), resulting in a mild HSCR phenotype (lack of the ENS limited to the distal colon) (17), were comparable to those in littermate WT mice (Fig. S3). These results demonstrate that early-onset syndromic deafness develops in c-Ret-KI$^{Y1062F/Y1062F}$ mice with severe HSCR (6) but not in c-Ret-KI$^{S697A/S697A}$ mice with mild HSCR (17).

Neurodegeneration of SGNs in c-Ret-KI$^{Y1062F/Y1062F}$ Mice. We next performed morphological analyses of Y1062-mediated congenital deafness. The number of c-Ret protein–expressed SGNs in c-Ret-KI$^{Y1062F/Y1062F}$ mice and that in littermate WT mice were no different on P14 (Fig. 3*A Upper*). The number of Y1062-phosphorylated SGNs was undetectably small in c-Ret-KI$^{Y1062F/Y1062F}$ mice, even on P14, compared with that in WT mice on P14 (Fig. 3 *A Lower* and *B*). Cell density of SGNs in the basal turn in c-Ret-KI$^{Y1062F/Y1062F}$ mice on P8 and P14 was 20–35% lower than that in the basal turn in littermate WT mice (Fig. 3 *C Lower* and *D*), although those on P2.5 were comparable in c-Ret-KI$^{Y1062F/Y1062F}$ mice and littermate WT mice (Fig. 3 *C Upper* and *D*). We further

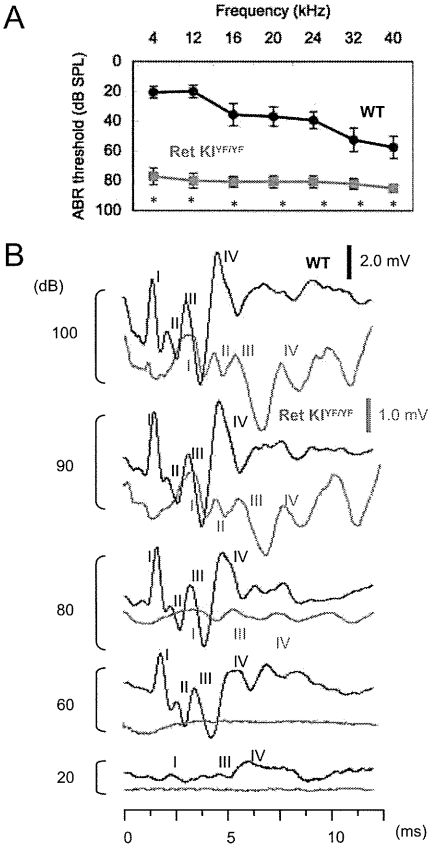

Fig. 2. Congenital deafness in c-Ret-KI$^{Y1062F/Y1062F}$ mice. (*A*) Hearing levels (mean ± SE) in 18-d-old c-Ret-KI$^{Y1062F/Y1062F}$ mice (Ret KI$^{YF/YF}$, red squares, $n = 8$) and littermate WT mice (WT, black circles, $n = 8$) measured by ABR. Significant difference ($^*P < 0.01$) from the control was analyzed by the Mann–Whitney *U* test. (*B*) ABR waveforms of 18-d-old littermate WT mice (black line) and c-Ret-KI$^{YF/YF}$ mice (red line) at 20- to 100-dB SPL at 4 kHz are presented at different scales (WT, 2.0 mV; c-Ret-KI$^{YF/YF}$ mice, 1.0 mV) for clarity. The peaks of ABR waves I, II, III, and IV are indicated. The absolute latencies of all four ABR waves and the interpeak latencies for waves I–II (auditory nerve) at 100 dB were significantly increased in c-Ret-KI$^{YF/YF}$ mice as follows: wave I (WT: 1.52 ms vs. c-Ret-KI$^{YF/YF}$ mice: 3.18 ms), wave II (WT: 2.23 ms vs. c-Ret-KI$^{YF/YF}$ mice: 4.36 ms), wave III (WT: 3.24 ms vs. c-Ret-KI$^{YF/YF}$ mice: 5.58 ms), wave IV (WT: 4.86 ms vs. c-Ret-KI$^{YF/YF}$ mice: 7.43 ms), and waves I–II (WT: 0.82 ms vs. c-Ret-KI$^{YF/YF}$ mice: 1.21 ms).

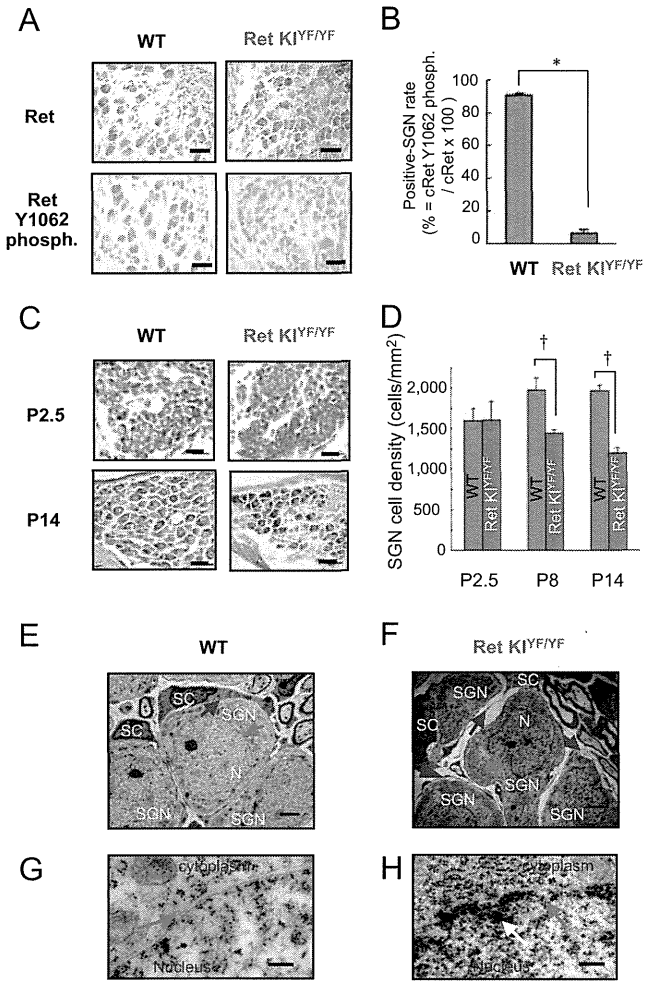

Fig. 3. Neurodegeneration of SGNs in c-Ret-KI$^{Y1062F/Y1062F}$ mice. (*A*) Immunohistochemical analyses for serial sections of the levels of c-Ret expression (*Upper*) and its phosphorylated Y1062 (*Lower*) in SGNs from 14-d-old littermate WT mice (WT, *Left*) and c-Ret-KI$^{Y1062F/Y1062F}$ mice (Ret KI$^{YF/YF}$, *Right*). (*B*) Percentage (mean ± SE) of Y1062-phosphorylated (phosph.) SGNs from 14-d-old c-Ret-KI$^{Y1062F/Y1062F}$ mice (Ret KI$^{YF/YF}$, red bar, $n = 3$) and littermate WT mice (WT, blue bar, $n = 3$). (Scale bars: 20 μm.) (*C*) Morphological analysis of SGNs from 2.5-d-old (*Upper*) and 14-d-old (*Lower*) WT mice (WT, *Left*) and littermate c-Ret-KI$^{Y1062F/Y1062F}$ mice (Ret KI$^{YF/YF}$, *Right*) by Kluver–Barrera staining. (*D*) Cell density (mean ± SE) of SGNs from 2.5-d-old (P2.5), 8-d-old (P8), and 14-d-old (P14) c-Ret-KI$^{Y1062F/Y1062F}$ mice (Ret KI$^{YF/YF}$, red bar, $n = 3$) and littermate WT mice (WT, blue bar, $n = 3$). (Scale bars: 20 μm.) The method for staining and estimating the percentage and cell density is described in detail in *Materials and Methods*. Significant difference ($^*P < 0.01$; $^\dagger P < 0.05$) from the control was analyzed by the Mann–Whitney *U* test (*B* and *D*). (*E–H*) TEM for SGNs from 14-d-old c-Ret-KI$^{Y1062F/Y1062F}$ mice (Ret KI$^{YF/YF}$, *F* and *H*) and littermate WT mice (WT, *E* and *G*). (*E* and *F*) Gap areas (blue arrows in *F*) between SGNs (SGN in *F*) with shrunken nuclei (red arrow in *F*) and Schwann cells (SC in *F*) were observed in c-Ret-KI$^{Y1062F/Y1062F}$ mice but not in littermate WT mice (blue arrow in *E*). N, nucleus. (*G* and *H*) Shrunken nuclei of SGNs with discontinuous nuclear membrane (red arrow in *H*) from c-Ret KI$^{Y1062F/Y1062F}$ mice and intact nuclear membrane of SGNs from WT mice (red arrow in *E* and *G*). The yellow arrow in *H* indicates condensed heterochromatin in the peripheral area of the nucleus of SGNs from c-Ret KI$^{Y1062F/Y1062F}$ mice. (Scale bars: *E* and *F*, 2 μm; *G* and *H*, 500 nm.)

performed detailed morphological analyses of SGNs from c-Ret-KI$^{Y1062F/Y1062F}$ mice during the hearing developmental stage by transmission electron microscopy (TEM) (Fig. 3 *E–H*). SGNs in c-Ret-KI$^{Y1062F/Y1062F}$ mice on P14 exhibited shrunken nuclei (Fig. 3*F*, red arrow) with discontinuous nuclear membranes (Fig. 3*H*, red arrow) and highly condensed heterochromatin in the peripheral area (Fig. 3*H*, yellow arrow), whereas those in littermate WT mice had intact bilayer membranes of nuclei (Fig. 3 *E* and *G*, red arrows). c-Ret-KI$^{Y1062F/Y1062F}$ mice on P14 also showed gaps between SGNs and Schwann cells (Fig. 3*F*, blue arrows) compared with those in littermate WT mice (Fig. 3*E*, blue arrow). On the other hand, no hallmarks for apoptotic signals in SGNs were found in either c-Ret-KI$^{Y1062F/Y1062F}$ mice or littermate WT mice on P8, P12, and P14 (Fig. S4).

Congenital Hearing Loss in c-Ret-KI$^{Y1062F/Y1062F}$ Mice Was Rescued by Introducing Constitutively Activated RET. We then tried to rescue the congenital hearing loss in c-Ret-KI$^{Y1062F/Y1062F}$ mice. For this purpose, we crossed c-Ret-KI$^{Y1062F/Y1062F}$ mice with constitutively activated RET (RFP-RET)-carrying transgenic mice (RET-Tg mice) of line 242 (18) and established c-Ret-KI$^{Y1062F/Y1062F}$;RET-Tg mice. Congenital hearing loss was again observed in 21-d-old c-Ret-KI$^{Y1062F/Y1062F}$ mice (Fig. 4*A*, red squares, and Fig. S5*B*). Hearing levels in c-Ret-KI$^{Y1062F/Y1062F}$;RET-Tg mice were comparable to those in littermate WT mice and were significantly improved compared with those in littermate c-Ret-KI$^{Y1062F/Y1062F}$ mice (Fig. 4*A* and Fig. S5). Correspondingly, the number of Y1062-phosphorylated SGNs in c-Ret–expressed SGNs and cell density of SGNs from c-Ret-KI$^{Y1062F/Y1062F}$;RET-Tg mice were comparable to those from littermate WT mice and significantly higher than those from c-Ret-KI$^{Y1062F/Y1062F}$ mice (Fig. 4 *B–E*). On the other hand, results of a previous study in vitro (19) and our results (Fig. S6) suggested that phosphorylated levels of Y1062 in c-RET modulate NF-κB activities via AKT phosphorylation levels in neural cells. In addition, impairments of NF-κB–mediating signaling have been shown to cause down-regulation of calbindin D28k, which contributes to neuronal survival, leading to neurodegenerative disorders (20). Our results and the results of previous studies mentioned above encouraged us to determine immunohistochemically the phosphorylation levels of NF-κB and Akt and the expression levels of calbindin D28k in SGNs from c-Ret-KI$^{Y1062F/Y1062F}$ mice to analyze the etiology of c-Ret–mediated congenital hearing loss further. Results of this study in vivo showed that not only phosphorylation levels of NF-κB and Akt but expression levels of calbindin D28k were impaired in SGNs from c-Ret-KI$^{Y1062F/Y1062F}$ mice and were restored in SGNs from c-Ret-KI$^{Y1062F/Y1062F}$;RET-Tg mice (Fig. 5).

Discussion

In this study, we provide direct evidence that c-*Ret* is a congenital deafness-related molecule in mice. Our results partially correspond to results of previous studies showing that GDNF has a protective effect on antibiotics-induced ototoxicities (21–24). Mutation of c-Ret at Y1062 has been shown to fail to respond to GDNF in vitro (19). However, previous studies have indicated that there is a Ret-independent signaling pathway stimulated by GDNF (5, 8, 25). Moreover, it has not been determined whether impairment of c-Ret kinase activity affects hearing, even though it has been shown that c-Ret, GFRα1, and GDNF are expressed in auditory neurons (26, 27). Our results strongly suggest that impaired phosphorylation of Y1062 in c-Ret without change in the expression level results in the development of congenital hearing loss with neurodegeneration of SGNs in mice. We further demonstrated congenital hearing loss in human patients with c-*RET*–mediated HSCR. Thus, this study indicated the importance of considering the activity as well as the expression of the target molecule to elucidate the etiologies of hereditary deafness.

This study demonstrated that c-Ret-KI$^{Y1062F/Y1062F}$ mice had severe congenital deafness with neurodegeneration of SGNs, resulting in decreased numbers of SGNs on P8–18 (Figs. 2 and 3). In contrast, the number and morphology of SGNs were comparable between c-Ret-KI$^{Y1062F/Y1062F}$ mice and WT mice on P2–3 (Fig. 3 *C* and *D*). These results suggest that SGNs even from c-Ret-KI$^{Y1062F/Y1062F}$ mice developed normally at least until P3, when

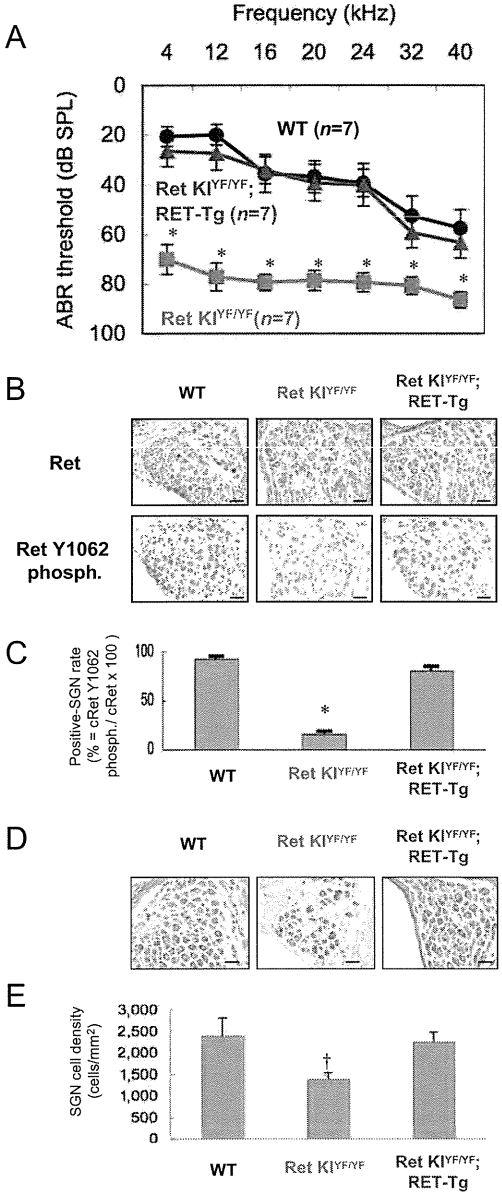

Fig. 4. Rescue of congenital hearing loss in c-Ret-KI$^{Y1062F/Y1062F}$ mice by introducing constitutively activated RET. (*A*) Hearing levels (mean ± SE) in 21-d-old WT mice (WT, black circles, $n = 7$), littermate c-Ret-KI$^{Y1062F/Y1062F}$ mice (Ret KI$^{YF/YF}$, red squares, $n = 7$), and c-Ret-KI$^{Y1062F/Y1062F}$;RFP/RET mice (Ret KI$^{YF/YF}$;RET-Tg, blue triangles, $n = 7$) mice measured by ABR. (*B*) Immunohistochemical analyses for serial sections of the levels of c-Ret expression (*Upper*) and its phosphorylated (phosph.) Y1062 (*Lower*) in SGNs from 15-d-old mice of three different strains (WT, Ret KI$^{YF/YF}$, and Ret KI$^{YF/YF}$;RET-Tg). (Scale bars: 20 μm.) (*C*) Percentages (mean ± SE) of Y1062-phosphorylated SGNs from littermate 15-d-old mice of three different strains (WT, Ret KI$^{YF/YF}$, and Ret KI$^{YF/YF}$;RET-Tg) are presented. (*D*) Morphological analysis of SGNs from 15-d-old mice of three different strains (WT, Ret KI$^{YF/YF}$, and Ret KI$^{YF/YF}$;RET-Tg) with Kluver–Barrera staining. (Scale bars: 20 μm.) (*E*) Cell density (mean ± SE) of SGNs from three mice of each mouse strain is presented. The method for staining and estimating the percentage and the cell density is described in detail in *Materials and Methods*. Significant difference ($^*P < 0.01$; $^\dagger P < 0.05$) from the control was analyzed by the Kruskal–Wallis *H* test (*A, C, and E*).

Y1062 phosphorylation in c-Ret of SGNs from WT mice was undetectable, but those from c-Ret-KI$^{Y1062F/Y1062F}$ mice no longer survived on P8–18, when the level of Y1062 phosphorylation in c-Ret of SGNs from WT mice was high (summarized in Fig. S7 *A–C*). Y1062 phosphorylation in c-Ret has been reported to mediate

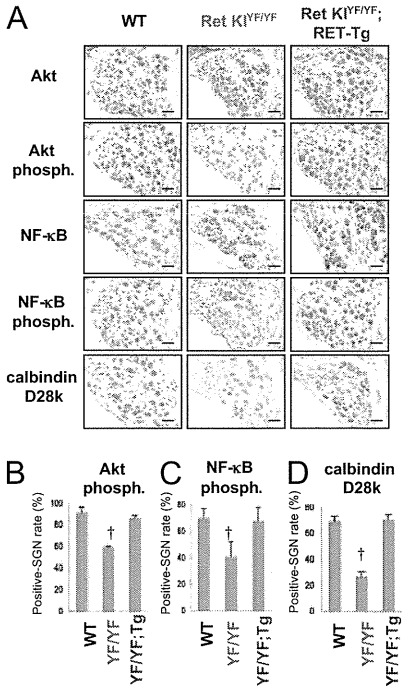

Fig. 5. Immunohistochemical analyses of phosphorylation levels of NF-κB and Akt and expression levels of calbindin D28k in SGNs from c-Ret-KI$^{Y1062F/Y1062F}$ mice. (*A*) Immunohistochemical analyses of SGNs from 15-d-old WT mice, littermate c-Ret-KI$^{Y1062F/Y1062F}$ mice (Ret KI$^{YF/YF}$) and c-Ret-KI$^{Y1062F/Y1062F}$;RFP/RET mice (Ret KI$^{YF/YF}$;RET-Tg) with polyclonal antibodies against Akt, phosphorylated Akt (Akt phosph.), NF-κB, phosphorylated NF-κB (NF-κB phosph.), and calbindin D28k. All specimens were developed with diaminobenzidine, followed by counterstaining with hematoxylin. (Scale bars: 20 μm.) (*B–D*) Percentage of positive SGN number (mean ± SE) of phosphorylated Akt (*B*), phosphorylated NF-κB (*C*), and calbindin D28k (*D*) in WT mice, littermate c-Ret-KI$^{Y1062F/Y1062F}$ mice (YF/YF), and c-Ret-KI$^{Y1062F/Y1062F}$;RFP/RET mice (YF/YF;RET-Tg) is presented. The method for estimating the percentage is described in detail in *Materials and Methods*. Significant difference ($^\dagger P < 0.05$) from the control was analyzed by the Kruskal–Wallis *H* test in *B–D*.

several biological responses, including survival of neuronal cells (8, 19). We therefore conclude that complete impairment of Y1062 phosphorylation in c-Ret affects survival of SGNs during the late stage of hearing development after birth in mice (around P8–18).

Our results further demonstrated that c-Ret–mediated congenital hearing loss involves impaired activities of Akt and NF-κB, with impaired expression of calbindin D28k in SGNs (Fig. 5). The impairments of these molecules in SGNs from c-Ret-KI$^{Y1062F/Y1062F}$ mice were clearly rescued by introducing constitutively activated RET (Fig. 5). These results partially correspond to results of a previous study in vitro and in vivo showing that GDNF induces expression of calbindin D28k, which promotes neural survival, via Akt/NF-κB signaling in substantia nigra neurons (28). Thus, our results suggest a mechanistic model for c-Ret–mediated congenital deafness in which impairments of the c-Ret–mediated signaling pathway cause decreased expression of calbindin D28k via Akt/NF-κB signaling, resulting in auditory nerve degeneration (summarized in Fig. S7 *D* and *E*). The neurodegeneration of SGNs from c-Ret-KI$^{Y1062F/Y1062F}$ mice did not involve the hallmark of apoptotic signals (Fig. S4). The results of a previous study also showed that neurodegeneration of postmigratory enteric neurons did not involve apoptotic signals during the developmental stage in mice with conditional ablation of c-*Ret* (29).

Hearing losses in three patients with HSCR were previously reported (30). Because the causal genes in patients who have HSCR have not been identified, we performed mutational anal-

ysis in this study for *RET*, *GDNF*, *neurturin* (*NTN*), *SOX10*, *EDNRB*, and *endothelin 3* (*ET-3*) genes of patients with HSCR, as listed in Table S1. We found that the patients with HSCR who have hearing losses have mutations only in RET among the above genes (Fig. S8 and Table S1). The results obtained with c-*Ret* KI mice demonstrate that impairments of Y1062 phosphorylation in c-Ret cause congenital hearing loss (Fig. 2 and 4), whereas normal hearing is maintained with even complete impairment of S697 phosphorylation in c-Ret (Fig. S3). In humans, we found hearing impairments in three patients with severe HSCR, including two male patients with homozygous and heterozygous mutations at arginine 969 located in c-RET kinase domains and one male patient with a nucleotide deletion at *RET* codon 13, resulting in a frameshift and termination at codon 22. No hearing impairments were found in patients with other heterozygous missense mutations at codons 30, 144, 489, 734, 897, and 942 (Table S1). Therefore, these results suggest that impairments of c-*Ret* and c-*RET* cause hearing losses in mice and humans in a site-dependent manner. Further study is needed to determine the correlation between mutational sites of c-*Ret* and c-*RET* and hearing losses in mice and humans.

We finally demonstrated that congenital hearing loss involving neurodegeneration of SGNs in c-Ret-KI$^{Y1062F/Y1062F}$ mice was rescued by introducing constitutively activated RET (Figs. 4 and 5). Despite a significantly increased risk for syndromic deafness in patients with HSCR (11, 12), no effective therapies for deafness have been established. Therefore, our findings will be useful for the development of therapeutical strategies targeting c-RET kinase against hearing impairments.

Materials and Methods

Mice. c-Ret-KI$^{Y1062F/Y1062F}$ mice (6), c-Ret-KI$^{S697A/S697A}$ mice (17), and RET-Tg mice of line 242 (18) were previously reported. There are no reports about hearing levels in these strains except a previous report showing that hearing levels in 10-wk-old RET-Tg mice and littermate WT mice were comparable (31). In this study, c-Ret-KI$^{Y1062F/+}$;RET-Tg mice were newly established by crossing the c-Ret-KI$^{Y1062F/+}$ mouse with the RET-Tg mouse. All experiments were authorized by the Institutional Animal Care and Use Committee of Chubu University (approval no. 2210038) and the Institutional Recombinant DNA Experiment Committee of Chubu University (approval no. 06-01) and followed the Japanese Government Regulations for Animal Experiments.

Measurement of Hearing. ABR measurements (AD Instruments Pty. Ltd.) were performed as described previously (30, 32). Tone burst stimuli were measured at 5 dB stepwise from 0-dB SPL to 70- or 90-dB SPL. The threshold was obtained by identifying the lowest level of I wave of ABR recognized. Data are presented as mean ± SE.

Morphological Analysis with a Light Microscope. After perfusion fixation with Bouin's solution, cochleae from 0.5- to 21-d-old mice were immersed in the same solution overnight and for 1 wk, respectively. Kluver–Barrera staining was performed with paraffin sections. Immunohistochemical analyses with polyclonal antibodies against c-Ret protein (1:150; Immuno Biological Laboratories), phosphorylated c-Ret Y1062 (1:150) (33), Akt (1:300; Cell Signaling), phosphorylated Akt (1:50; Cell Signaling), and phosphorylated NF-κB p50 (1:50; Santa Cruz) were performed on frozen sections with Can Get Signal immunostaining solution (TOYOBO). Immunohistochemical analysis with polyclonal antibodies against NF-κB p50 (1:100; Santa Cruz) and calbindin D28k (1:150; Chemicon) was performed for paraffin sections. For the detection of NF-κB p50, the paraffin sections were treated with 10 mM sodium citrate (pH 6.0) for 10 min at 90 °C for antigen retrieval. For the detection of calbindin D28k, the paraffin sections were treated with 10 mM sodium citrate (pH 6.0) for 10 min at 90 °C for antigen retrieval, and Can Get Signal immunostaining solution was used as dilution buffer. The VECTASTAIN ABC kit (Vector) and Envision kit/HRP (diaminobenzidine; DAKO) were used in each immunohistochemical analysis with counterstained hematoxylin. Immunohistochemical estimation of the percentage of positive SGNs detected by antibodies was calculated using the software program WinROOF (Mitani Corp.), as previously reported (34). In brief, the number of immunohistochemically positive SGNs was divided by the total number of SGNs in each Rosenthal's canal from three or four mice for each mouse strain. In total, 160–200 SGNs were counted for each evaluation of cell density and percentage. In the case of immunohistochemical estimation of phosphorylated protein, percentage (mean ± SE) was calculated by dividing the number of phosphorylated SGNs by the number of the protein-expressing SGNs in each Rosenthal's canal from three or four mice for each mouse strain. Estimation of the cell density of SGNs with Kluver–Barrera staining basically followed the previous method (35, 36). In brief, the area of Rosenthal's canal in five sections from each mouse was measured with the software program WinROOF. The cell density of SGNs from three or four mice for each mouse strain was calculated by dividing the cell number of SGNs in the measured Rosenthal's canal by the area. In total, 160–200 SGNs in five sections from each mouse were examined. In total, 160–200 SGNs were counted for each evaluation of cell density and percentage.

Morphological Analysis by TEM. Preparation of tissues for TEM basically followed the previous method (35). In brief, after perfusion fixation with a fixative solution I containing 2% (vol/vol) paraformaldehyde, 2% (vol/vol) glutaraldehyde and 0.3 M Hepes (pH 7.4), dissected murine cochleae were immersed in the same fixative solution overnight at 4 °C. The cochleae were then fixed with a fixative solution II containing 2% (vol/vol) osmium tetroxide and 0.3 M Hepes (pH 7.4) at 4 °C for 3 h. After rinsing off the fixative solution, the cochleae were dehydrated with a graded series of ethanol and embedded in epoxy resin (Quetol 651; Nisshin EM). Ultrathin sections (thickness = 70 nm) were observed under an electron microscope at 80 kV (JEM1200EX; JEOL).

Mutational Analysis in Patients with HSCR. We analyzed mutations of *RET*, *GDNF*, *NTN*, *SOX10*, *EDNRB*, and *ET-3* genes in DNA samples from 15 children with total colonic aganglionosis, as described previously (37). Amplification was accomplished with a reaction mixture containing 100 ng of lymphocyte DNA, 2.5 μM each set of primers, 200 μM dNTP, 10 mM Tris HCl (pH 8.3), 1.5 mM $MgCl_2$, 50 mM KCl, and 1.0 U of Taq DNA polymerase. Thermocycling conditions consisted of denaturation at 95 °C for 9 min, 45 cycles of annealing at 60 °C for 2 min, and extension at 95 °C for 30 s, followed by a denaturing step at 60 °C for 3 min in an automatic thermocycler (GeneAmp PCR System 2400; Perkin–Elmer). The DNA sequencings were carried out by the direct dyedeoxy terminator cycle method using a fluorescent automatic DNA sequencer (Model 373A DNA Sequencing systems; Applied Biosystems).

Ethical Considerations. The study was approved by the Ethics Committee of Chubu University (approval no. 20008-4) and conducted according to the Declaration of Helsinki. All patients gave voluntary written informed consent.

Statistics. Significant difference ($^{*}P < 0.01$; $^{\dagger}P < 0.05$) from the control was analyzed by the Mann–Whitney *U* test (Figs. 2 and 3) and the Kruskal–Wallis *H* test (Figs. 4 and 5).

ACKNOWLEDGMENTS. We thank Kyoko Ohgami, Yoko Kato, Yukie Ohtsuka, and Harumi Ohno for their technical assistance. We also thank Dr. Izumi Nakashima and the laboratory members for their helpful discussions. This study was supported in part by Grants-in-Aid for Scientific Research (B) Grants 19390168 and 20406003 (to M.K.) and Grants-in-Aid for Young Scientists (B) Grant 18790738 (to N.O.) and Grant 20791232 (to M.I.-E.) from the Ministry of Education, Culture, Sports, Science, and Technology; the COE Project for Private Universities (Grant S0801055) from the Ministry of Education, Culture, Sports, Science, and Technology; the Uehara Memorial Foundation (M.K.), Rohto Awards (M.K.), Chubu University Grants A (to N.O. and M. K.), B (to N.O.), and C (to M.K.); and the GCOE Project from the Ministry of Education, Culture, Sports, Science, and Technology (to M.T.).

1. Lalwani AK, Gürtler N (2008) Sensorineural hearing loss, the aging inner ear, and hereditary hearing impairment. *CURRENT Diagnosis and Treatment in Otolaryngology—Head and Neck Surgery*, ed Lalwani AK (McGraw–Hill, New York), 2nd Ed, pp 683–704.
2. Brown SD, Hardisty-Hughes RE, Mburu P (2008) Quiet as a mouse: Dissecting the molecular and genetic basis of hearing. *Nat Rev Genet* 9:277–290.
3. Gratton MA, Vázquez AE (2003) Age-related hearing loss: Current research. *Curr Opin Otolaryngol Head Neck Surg* 11:367–371.
4. Takahashi M (2001) The GDNF/RET signaling pathway and human diseases. *Cytokine Growth Factor Rev* 12:361–373.
5. Trupp M, Scott R, Whittemore SR, Ibáñez CF (1999) Ret-dependent and -independent mechanisms of glial cell line-derived neurotrophic factor signaling in neuronal cells. *J Biol Chem* 274:20885–20894.
6. Jijiwa M, et al. (2004) A targeting mutation of tyrosine 1062 in Ret causes a marked decrease of enteric neurons and renal hypoplasia. *Mol Cell Biol* 24:8026–8036.

7. Drosten M, Pützer BM (2006) Mechanisms of Disease: Cancer targeting and the impact of oncogenic RET for medullary thyroid carcinoma therapy. *Nat Clin Pract Oncol* 3: 564–574.
8. Airaksinen MS, Saarma M (2002) The GDNF family: Signaling, biological functions and therapeutic value. *Nat Rev Neurosci* 3:383–394.
9. Heanue TA, Pachnis V (2007) Enteric nervous system development and Hirschsprung's disease: Advances in genetic and stem cell studies. *Nat Rev Neurosci* 8:466–479.
10. Kato M, et al. (2002) Repair by Src kinase of function-impaired RET with multiple endocrine neoplasia type 2A mutation with substitutions of tyrosines in the COOH-terminal kinase domain for phenylalanine. *Cancer Res* 62:2414–2422.
11. Moore SW, Johnson AG (1998) Hirschsprung's disease: Genetic and functional associations of Down's and Waardenburg syndromes. *Semin Pediatr Surg* 7:156–161.
12. Moore SW (2006) The contribution of associated congenital anomalies in understanding Hirschsprung's disease. *Pediatr Surg Int* 22:305–315.
13. Attié T, et al. (1995) Mutation of the endothelin-receptor B gene in Waardenburg-Hirschsprung disease. *Hum Mol Genet* 4:2407–2409.
14. Pingault V, et al. (1998) SOX10 mutations in patients with Waardenburg-Hirschsprung disease. *Nat Genet* 18:171–173.
15. Schuchardt A, D'Agati V, Larsson-Blomberg L, Costantini F, Pachnis V (1994) Defects in the kidney and enteric nervous system of mice lacking the tyrosine kinase receptor Ret. *Nature* 367:380–383.
16. Rubel EW, Fritzsch B (2002) Auditory system development: Primary auditory neurons and their targets. *Annu Rev Neurosci* 25:51–101.
17. Asai N, et al. (2006) Targeted mutation of serine 697 in the Ret tyrosine kinase causes migration defect of enteric neural crest cells. *Development* 133:4507–4516.
18. Kato M, et al. (1999) Linkage between melanocytic tumor development and early burst of Ret protein expression for tolerance induction in metallothionein-I/ret transgenic mouse lines. *Oncogene* 18:837–842.
19. Hayashi H, et al. (2000) Characterization of intracellular signals via tyrosine 1062 in RET activated by glial cell line-derived neurotrophic factor. *Oncogene* 19:4469–4475.
20. Mattson MP, Camandola S (2001) NF-kappaB in neuronal plasticity and neurodegenerative disorders. *J Clin Invest* 107:247–254.
21. Suzuki M, et al. (2000) Effect of transgenic GDNF expression on gentamicin-induced cochlear and vestibular toxicity. *Gene Ther* 7:1046–1054.
22. Yagi M, et al. (2000) Spiral ganglion neurons are protected from degeneration by GDNF gene therapy. *J Assoc Res Otolaryngol* 1:315–325.
23. Liu Y, et al. (2008) Protection against aminoglycoside-induced ototoxicity by regulated AAV vector-mediated GDNF gene transfer into the cochlea. *Mol Ther* 16: 474–480.
24. Scheper V, et al. (2009) Effects of delayed treatment with combined GDNF and continuous electrical stimulation on spiral ganglion cell survival in deafened guinea pigs. *J Neurosci Res* 87:1389–1399.
25. Poteryaev D, et al. (1999) GDNF triggers a novel ret-independent Src kinase family-coupled signaling via a GPI-linked GDNF receptor alpha1. *FEBS Lett* 463:63–66.
26. Stöver T, Gong TL, Cho Y, Altschuler RA, Lomax MI (2000) Expression of the GDNF family members and their receptors in the mature rat cochlea. *Brain Res Mol Brain Res* 76:25–35.
27. Stöver T, Nam Y, Gong TL, Lomax MI, Altschuler RA (2001) Glial cell line-derived neurotrophic factor (GDNF) and its receptor complex are expressed in the auditory nerve of the mature rat cochlea. *Hear Res* 155:143–151.
28. Wang HJ, et al. (2008) Calbindin-D28K expression induced by glial cell line-derived neurotrophic factor in substantia nigra neurons dependent on PI3K/Akt/NF-kappaB signaling pathway. *Eur J Pharmacol* 595:7–12.
29. Uesaka T, Nagashimada M, Yonemura S, Enomoto H (2008) Diminished Ret expression compromises neuronal survival in the colon and causes intestinal aganglionosis in mice. *J Clin Invest* 118:1890–1898.
30. Shimotake T, Iwai N (1994) Auditory brainstem response in children with total intestinal aganglionosis. *Lancet* 343:1362.
31. Hayashi H, et al. (2004) A novel RFP-RET transgenic mouse model with abundant eumelanin in the cochlea. *Hear Res* 195:35–40.
32. Zheng QY, Johnson KR, Erway LC (1999) Assessment of hearing in 80 inbred strains of mice by ABR threshold analyses. *Hear Res* 130:94–107.
33. Yamamoto M, et al. (2001) Preserved phosphorylation of RET receptor protein in spinal motor neurons of patients with amyotrophic lateral sclerosis: An immunohistochemical study by a phosphorylation-specific antibody at tyrosine 1062. *Brain Res* 912:89–94.
34. Enomoto A, et al. (2009) Roles of disrupted-in-schizophrenia 1-interacting protein girdin in postnatal development of the dentate gyrus. *Neuron* 63:774–787.
35. Lang H, et al. (2006) Nuclear factor kappaB deficiency is associated with auditory nerve degeneration and increased noise-induced hearing loss. *J Neurosci* 26:3541–3550.
36. Shimada A, Ohta A, Akiguchi I, Takeda T (1992) Inbred SAM-P/10 as a mouse model of spontaneous, inherited brain atrophy. *J Neuropathol Exp Neurol* 51:440–450.
37. Inoue K, Shimotake T, Iwai N (2000) Mutational analysis of RET/GDNF/NTN genes in children with total colonic aganglionosis with small bowel involvement. *Am J Med Genet* 93:278–284.

Ischemia-Reperfusion Injury of the Cochlea: Pharmacological Strategies for Cochlear Protection and Implications of Glutamate and Reactive Oxygen Species

Keiji Tabuchi*, Bungo Nishimura, Shuho Tanaka, Kentaro Hayashi, Yuki Hirose and Akira Hara

Department of Otolaryngology, Graduate School of Comprehensive Human Sciences, University of Tsukuba, Tsukuba, Japan

Abstract: A large amount of energy produced by active aerobic metabolism is necessary for the cochlea to maintain its function. This makes the cochlea vulnerable to blockade of cochlear blood flow and interruption of the oxygen supply. Although certain forms of human idiopathic sudden sensorineural hearing loss reportedly arise from ischemic injury, the pathological mechanism of cochlear ischemia-reperfusion injury has not been fully elucidated. Recent animal studies have shed light on the mechanisms of cochlear ischemia-reperfusion injury. It will help in the understanding of the pathology of cochlear ischemia-reperfusion injury to classify this injury into ischemic injury and reperfusion injury. Excitotoxicity, mainly observed during the ischemic period, aggravates the injury of primary auditory neurons. On the other hand, oxidative damage induced by hydroxyl radicals and nitric oxide enhances cochlear reperfusion injury. This article briefly summarizes the generation mechanisms of cochlear ischemia-reperfusion injury and potential therapeutic targets that could be developed for the effective management of this injury type.

Keywords: Cochlea, Blood flow, Ischemia-reperfusion injury, Excitotoxicity, Oxidative damage.

INTRODUCTION

The sole purpose of the circulatory system is transportation. It performs oxygen and nutrient delivery and metabolic by-product removal. The labyrinthine artery is a terminal artery for cochlear blood supply. The cochlea is highly dependent on blood and oxygen supply to maintain its function. In animal models of cochlear ischemia, the cochlea becomes hypoxic or ischemic within one minute after occlusion of the labyrinthine artery.

It has been proposed that one of the major causes of human idiopathic sudden sensorineural hearing loss is impaired blood flow and oxygen delivery to the cochlea [1]. The aim of this review is to provide an overview of recent insights regarding the pathogenesis of cochlear ischemia-reperfusion injury observed in animal studies.

CHANGES IN COCHLEAR POTENTIALS AND MORPHOLOGIES DURING ISCHEMIA

Adenosine triphosphate (ATP), a critical compound in cellular energy metabolism, is synthesized in mitochondria from adenosine diphosphate (ADP) and inorganic phosphate in the presence of oxygen and nicotinamide adenine dinucleotide (NADH). Interruption of the blood supply causes ATP depletion in the cochlea [2]. If this ATP depletion during ischemia is severe, it may lead to the compromised function of all cochlear cells. Perlman *et al.* [3] were the first to perform an extensive study of functional and histological alterations of the cochlea during and after reversible cochlear ischemia in the guinea pig. Because the stria vascularis requires high-level energy supply to maintain endocochlear potential (EP) levels, EP rapidly declines immediately after the onset of ischemia to reach its lowest level (-30 to -40 mV). EP is essential to maintain the function of hair cells and cochlear afferent neurons, and its decrease results in the subsequent decrease of other cochlear potentials, such as cochlear microphonic (CM), distortion-product otoacoustic emission (DPOAE), and compound action potential (CAP) [4].

Generally, interruption of the blood supply causes various morphological changes including cellular, mitochondrial, and nuclear swelling, swelling of the endoplasmic reticulum, clearing of the cytoplasm, bleb formation, and the condensation of chromatin. However, the tolerance of cochlear cells to ischemia is variable among cell types. Dendrites of cochlear afferent neurons are one of the components most vulnerable to ischemia. The swelling of afferent neurons is observed in cases of cochlear ischemia of 5 minutes or longer. Ischemia-induced morphological changes are also observed in hair cells. Approximately 15 and 30 minutes of ischemia causes the swelling of outer and inner hair cells, respectively. As the ischemic period prolongs, more severe morphological changes are observed, such as the swelling of nuclei, bleb formation, and rupture of the cell membrane. Several hours of ischemia induces disintegration of the organ of Corti [4].

EXCITOTOXICITY OF COCHLEAR AFFERENT NEURONS DURING THE ISCHEMIC PERIOD

Excitotoxicity is an important and well-accepted theory proposed by Olney *et al.* [5], which explains one of the major pathophysiologies of brain ischemia. Excitotoxicity is

*Address correspondence to this author at the Department of Otolaryngology, Graduate School of Comprehensive Human Sciences, University of Tsukuba, 1-1-1 Tennodai, Tsukuba, 305-8575, Japan; Tel: +81-298-53-3147; Fax: +81-298-53-3147; E-mail: ktabuchi@md.tsukuba.ac.jp

1570-159X/10 $55.00+.00

caused by excessive amounts of glutamate in synaptic cleft. Glutamate is a putative excitatory neurotransmitter between inner hair cells and afferent neurons [6, 7]. Although vital for cochlear function, excessively released glutamate and the failure of its removal from synaptic clefts can lead to the excitotoxicity of cochlear afferent neurons due to the loss of ionic homeostasis. Puel *et al.* [8] showed that cochlear ischemia causes the excitotoxicity of afferent neurons to induce the massive swelling of afferent dendrites.

The excessive efflux of glutamate from inner hair cells results in cochlear excitotoxicity. Massive glutamate efflux in the perilymph of the cochlea is observed during cochlear ischemia [9, 10]. Besides this excessive efflux, the failed uptake of glutamate from the synaptic clefts into surrounding cells also causes cochlear excitotoxicity. To date, five subtypes of Na^+-dependent glutamate transporter: GLT-1, GLAST, EAAC1, EAAT4, and EAAT5, have been cloned [11-13]. Previous studies have demonstrated that GLAST is present in the supporting cells surrounding inner hair cells and in the satellite cells surrounding spiral ganglion neurons in the rodent cochlea [14, 15]. Takumi *et al.* [16] demonstrated the colocalization of GLAST and glutamine synthetase in supporting cells around inner hair cells. Based on their findings, it is suggested that glutamate released from the presynaptic region is taken into adjacent supporting cells using GLAST and then converted to glutamine in the supporting cells [17]. Glutamate transporters are required to terminate glutamate actions. Hakuba *et al.* [18] has shown that GLAST knockout mice are vulnerable to cochlear excitotoxicity. Although GLT-1 and EAAC1 also exist in the cochlea, the involvement of these glutamate transporters in cochlear exctitotoxicity has not yet been clarified.

It is now widely accepted that glutamate receptors fall into two major classes: the ionotropic receptors formed by ligand-gated cation channels and the metabotropic receptors that are coupled to G-proteins and act though intracellular chemical mechanisms [19-21]. Eight subtypes of metabotropic glutamate receptors have been currently identified, and subdivided into three groups according to sequence homology and response to agonists [22]. Ionotropic glutamate receptors are divided into three types: AMPA, kainite, and N-methyl-D-aspartate (NMDA) receptors. The swelling of afferent dendrites is induced *via* non-NMDA ionotropic glutamate receptors in the cochlea because the application of APMA and kainic acid to the cochlea leads to the same swelling of afferent dendrites. An AMPA/kainate receptor antagonist, 6-7-dinitroquinoxaline-2,3-dione (DNQX), protected most of the radial dendrites from the ischemia-induced swelling [8]. In contrast to the involvement of AMPA/kainate receptors in the cochlear excitotoxicity and cochlear ischemic injury, a definitive role of metabotropic and NMDA receptors in cochlear ischemic injury has not been shown. MK-801 and D-2-amino-5-phosphonopentanoate, NMDA receptor antagonists, did not show protective effects against cochlear ischemia [5, 23].

It is now considered that the excitotoxicity of cochlear afferent neurons often induces temporary hearing threshold shifts [24]. However, Sun *et al.* [25] demonstrated that some cochlear excitotoxicity might induce irreversible cochlear lesions because the number of cochlear ganglion neurons decreased after exposure to high concentration of kainic acid.

The swelling of afferent neurons is observed in cases of cochlear ischemia of 5 minutes or longer. Excitotoxicity is undoubtedly one of the leading causes of cochlear afferent neuron injury during ischemia (Fig. **1**).

CHARACTERISTICS OF COCHLEAR INJURY DURING THE REPERFUSION PERIOD

Although the cochlear response to ischemia has been extensively studied, the effects of reperfusion on the cochlea have recently received new attention. Recent animal models of cochlear ischemic injury are suitable to examine the time course of cochlear functions during reperfusion [9, 26-29]. The CAP threshold representing the function of cochlear afferent neurons gradually improved during the reperfusion period. On the other hand, DPOAE (representing the function of outer hair cells) initially recovered with time until 20 minutes after the onset of reperfusion when the cochlear circulation was restored. Thereafter the amplitude of DPOAE gradually decreased toward the noise level, whereas CAP gradually improved during this time period, as mentioned above. CM, another indicator of hair cell function, exhibited essentially the same time course during the reperfusion period as DPOAE [4]. Based on these findings, it is considered that the main lesion of cochlear reperfusion injury is in outer hair cells. In morphological studies of the cochlea, reperfusion of the cochlea induces swelling of the outer hair cells and eventual rupture of the outer hair cell membrane and nucleus [4]. The swelling of terminals of afferent dendrites improved during the reperfusion period [4]. This morphological finding is in agreement with the fact that CAP gradually improved whereas DPOAE decreased during reperfusion. Excitotoxicity during ischemia is involved in the swelling of afferent neurons, which improved during reperfusion. It has been shown that the glutamate concentration in the perilymph, which increased during the ischemic period, decreased toward the pre-ischemia level upon reperfusion [10].

INVOLVEMENT OF REACTIVE OXYGEN SPECIES IN REPERFUSION INJURY OF THE COCHLEA

As described in a previous section, outer hair cells functionally and structurally deteriorate during the early reperfusion period. Recent studies have indicated that free radicals such as hydroxyl radicals and nitric oxide (NO) are involved in the injury of outer hair cells.

It has been generally accepted that reoxygenation causes the accumulation of superoxide anions in tissues. The superoxide anion is converted by superoxide dismutase to hydrogen peroxide, which is relatively unreactive toward most organic molecules. However, the hydroxyl radical, a potent oxidant capable of promoting oxidative damage, may be generated by the reaction of hydrogen peroxide with iron (Fenton reaction). Hydroxyl radicals can oxidize DNA, proteins, and structural polymers including hyaluronic acid. In addition, they induce the peroxidation of polyunsaturated fatty acid, which damages biological membranes [30].

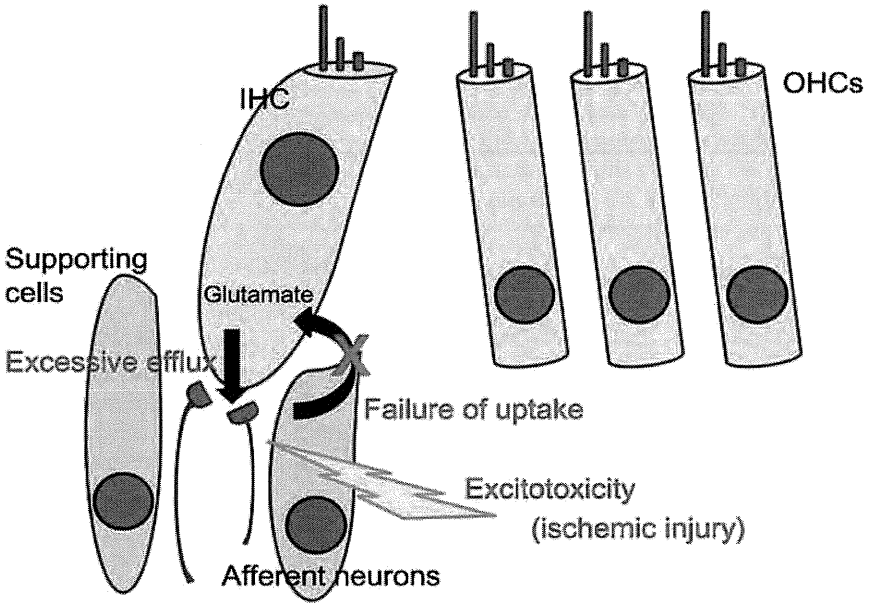

Fig. (1). Schematic view of cochlear ischemic injury. Glutamate is a putative neurotransmitter between inner hair cells and afferent neurons. Glutamate released from inner hair cells is promptly taken into the inner hair cells and supporting cells by glutamate transporters in the normal cochlea. Ischemia induces the excessive efflux of glutamate and dysfunction of the glutamate transporter. These cause the excitotoxicity of afferent neurons. IHC: inner hair cell. OHCs: outer hair cells.

Hypoxia increased the iron concentration in the perilymph of the cochlea [31], and the marked production of hydroxyl radicals was demonstrated during the re-oxygenation phase after hypoxia [32]. These findings suggest that hydroxyl radicals were generated *via* the Fenton reaction during the early reperfusion period in cochlear ischemia-reperfusion injury.

Generally, the main source of superoxide anions during reperfusion is considered to be mitochondria. Reduced intermediates of mitochondrial electron transport systems accumulate during ischemia and are oxidized during reperfusion (by reoxygenation), leading to the production of superoxide anions. Another potential source of superoxide anions is xanthine oxidase, which oxidizes hypoxanthine to xanthine and xanthine to urate. However, xanthine oxidase may not be involved in the generation of free radicals because allopurinol and oxypurinol, potent inhibitors of xanthine oxidase, did not exhibit any effect on cochlear ischemia-reperfusion injury [33].

Nitric oxide (NO) is also involved in the generation mechanism of cochlear ischemia-reperfusion injury. Transient ischemia causes a marked increase of NO production in the perilymph in the reperfusion period [34]. To date, three isoforms of NO synthase (NOS) have been distinguished: neuronal NOS (nNOS), endothelial NOS (eNOS), and inducible NOS (iNOS). The constitutive isoforms of NOS (i.e., nNOS and eNOS), but not iNOS are expressed in the normal cochlea [35, 36]. Recent findings suggest that NO generated by nNOS and iNOS deteriorates the cochlea in ischemia-reperfusion injury [29, 37, 38]. NO synthesized by iNOS plays a deleterious role in cerebral ischemia, and ischemia-induced iNOS mRNA expression and iNOS activity were delayed by several hours (more than 6) after transient cerebral ischemia [39, 40]. The administration of aminoguanidine, an iNOS inhibitor, decreased the postischemic shift of the ABR or CAP threshold at 1 to 5 days after 60-minute ischemia, but not at 4 hours after ischemia [29, 38]. These results strongly suggest that NO generated by nNOS and by iNOS aggravates cochlear injury in early and late phases of reperfusion, respectively (Fig. **2**).

TIME THRESHOLD OF ISCHEMIA TO INDUCE COCHLEAR DYSFUNCTION

Individual tissues have quite variable oxygen requirements. For example, the brain cannot tolerate hypoxia for more than a few minutes without permanent injury, although skeletal muscles can tolerate severe hypoxia or ischemia for several hours [41]. Several researchers have examined the time threshold of ischemia to induce cochlear dysfunction using animal models. EP and other cochlear potentials start to decrease within a minute after the cochlea is subjected to ischemia. When circulation is resumed, cochlear functions fully recover if the ischemic period is less than 10 minutes. However, DPOAE significantly decreases after ischemia of 10 minutes compared with the preischemic level [26]. CAP thresholds also elevate after ischemia of 10 minutes or longer [28]. These findings support the idea that ischemia of 10 minutes or longer at least transiently elevates the hearing threshold. When cochlear functions are followed for long periods after the onset of recirculation, ischemia of 15 to 30 minutes duration induces hair cell loss and permanent cochlear dysfunction [9, 29].

PHARMACOLOGICAL STRATEGIES TO PROTECT THE COCHLEA AGAINST ISCHEMIA-REPERFUSION INJURY

This section presents a brief overview of experimental data concerning pharmacological strategies for cochlear protection against ischemia-reperfusion injury.

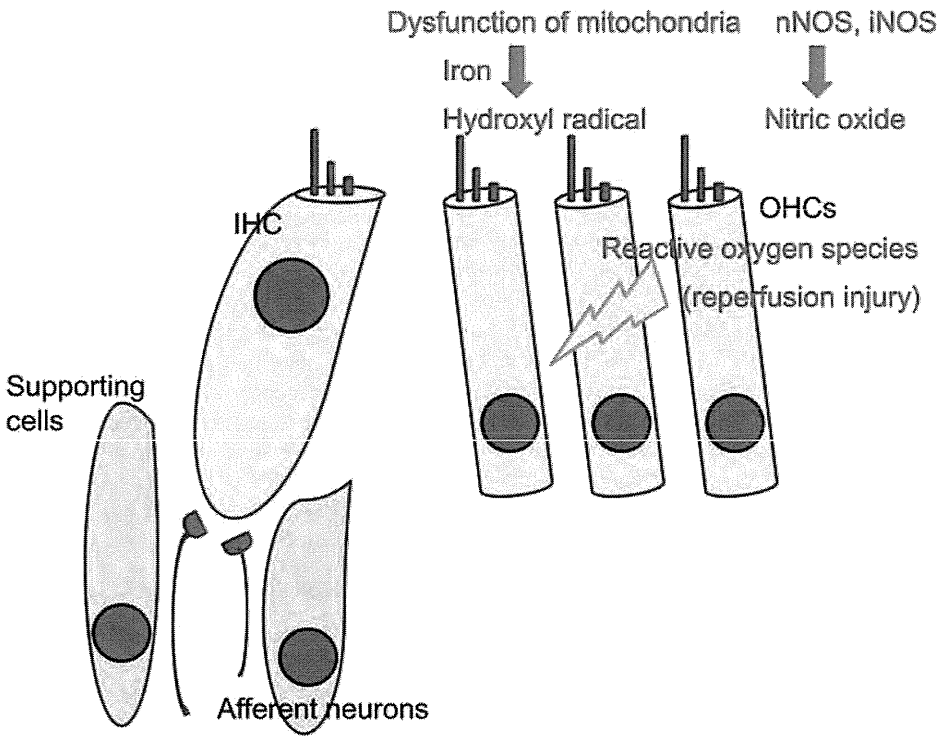

Fig. (2). Schematic view of cochlear reperfusion injury. Reoxygenation leads to the generation of superoxide anions, in which mitochondrial dysfunction may be involved. Superoxide anions are converted into hydroxyl radicals *via* the Fenton reaction in the presence of iron. NO is also generated by nNOS and iNOS during the reperfusion period. These reactive oxygen species cause the reperfusion injury of outer hair cells. IHC: inner hair cell. OHCs: outer hair cells.

1. Excitotoxicity

An AMPA/kainate receptor antagonist, 6-7-dinitroquinoxaline-2,3-dione (DNQX), protected most radial dendrites from ischemia-induced swelling [8]. In contrast to the protective effect of AMPA/kainate receptor inhibitors against cochlear excitotoxicity and cochlear ischemic injury, specific NMDA receptor antagonists including MK-801 and D-2-amino-5-phosphonopentanoate did not show any protective effect against cochlear ischemia [8, 23].

There are several agents reported to reduce cochlear excitotoxicity including a GABA(A) agonist (muscimol [24]), dopamine [42, 43], riluzole [44], ebselen [45], and pituitary adenyl cyclase-activating polypeptide (PACAP) [46]. Because the excitotoxicity of cochlear afferent neurons often induces temporary hearing threshold shifts [24], these agents are potential therapeutic targets to prevent temporary hearing deterioration.

The majority of clinical trials of glutamatergic antagonists were conducted in the fields of stroke, traumatic brain injury and dementia. However, treatment with glutamatergic antagonists failed to obtain even modest beneficial results, and those clinical trials were interrupted [47]. In addition, the adverse effect profile of glutamatergic antagonists has been described. Based on the findings obtained in central nervous system disorders, it seems reasonable to consider local application of glutamatergic antagonists for prevention of temporary elevation of hearing thresholds.

2. Free Radical Scavengers and NOS Inhibitors

Seidman and Quirk [48] first demonstrated the involvement of free radicals in cochlear ischemia-reperfusion injury. Since their report, several free radical scavengers have been reported to protect against cochlear ischemia-reperfusion injury, including U74006F, mannitol, edaravone, and dimethylthiourea [4, 28, 48, 49].

It has been suggested that superoxide and hydrogen peroxide have a limited reactivity with most biological molecules *in vivo*, and their interaction in the presence of a transition metal (e.g., iron) forms far more reactive hydroxyl radicals by the iron-catalyzed Haber-Weiss (Fenton) reaction that contribute to tissue injury [30]. The protective effects of deferoxamine, an iron chelator, in cochlear ischemia have been established [38, 50].

In addition to free radical scavengers and iron chletors, NOS inhibitors protect the cochlea. N-nitro-L-arginine decreased the postischemic CAP threshold shift [28]. Inhibitors of nNOS (7-nitroindazole, 3-bromo-7-nitroindazole) and iNOS (aminoguanidine) also protect the cochlea against ischemia-reperfusion injury [29, 38, 50].

Outer hair cells deteriorate during reperfusion, and cochlear reperfusion injury is most evidently observed in outer hair cells. DPOAE studies demonstrated that free radical scavengers, iron chelators, and NOS inhibitors protected outer hair cells from reperfusion injury [4, 50].